Neuromodulatory Mechanisms in the Auditory Tectothalamic Pathway

by

Luis Rivera

A dissertation submitted in partial fulfillment
of the requirements for the degree of
Doctor of Philosophy
(Neuroscience)
in the University of Michigan
2023

Doctoral Committee:

Assistant Professor Michael T. Roberts, Chair
Assistant Professor Pierre Apostolides
Associate Professor Sara Aton
Associate Professor R. Keith Duncan
Assistant Professor Kevin Jones
Professor Geoffrey Murphy

Luis Rivera

riluis@umich.edu

ORCID iD: 0000-0002-5898-1759

Dedication

Para Miguel y Carmen. Todo lo que mis hermanos y yo hemos logrado es gracias a ustedes.

Acknowledgements

First, I would like to thank my mentor, Dr. Michael T. Roberts, for believing in me from the moment I stepped into his lab. His guidance and mentorship have been invaluable in my formation as a scientist and a person. I could not have asked for a better mentor on this journey. Thank you to all my dissertation committee members for helping me think about my research beyond what I could see every time we met. I am very grateful for the amazing people I met and worked with in the Roberts Lab. I cherish all our moments together, in the lab and outside of research. I admire them all and will be expecting great things from each of them in the future. To the NGP staff, thank you for the many conversations about work, life, and everything in between. Every one of them helped keep me sane during this process, and I am so grateful for their willingness to move mountains for all their NGP students. I am grateful for Dr. Edu Suárez and Dr. James Porter. Their guidance at the University of Puerto Rico at Ponce and the Ponce Health Sciences University provided the foundation that I needed to achieve my scientific and career goals. To my friends in THE Cohort, thank you for all the support and friendship. Finally, I want to thank my family. Even when they had no idea what I wanted to do by moving to Michigan, all of them supported me and had my back every step of the way, no questions asked. The excitement of telling them my new results or good news about funding kept me motivated these past years.

Table of Contents

List of Figures

Abstract

How our brains identify and respond to speech and other auditory cues remains unclear. Neuromodulators, neurotransmitters known to affect the excitability of neurons by regulating processes such as neurotransmitter release from presynaptic terminals, are likely to modulate the excitability of neurons during sensory processing. In this dissertation, I aim to determine the roles and mechanisms of two distinct neuromodulators in two regions of the auditory pathway, the inferior colliculus (IC) and the medial geniculate (MG). My goal is to expand our knowledge on the role of neuromodulation in the auditory system.

The IC, a hub for auditory processing located in the midbrain, contains neurons that exhibit selective responses to different features of speech and sounds. Previous findings suggest that acetylcholine (ACh), a neuromodulator associated with attention and synaptic plasticity, may provide an attention-based mechanism to alter auditory processing in the IC. Furthermore, neurons in the IC express different combinations of nicotinic acetylcholine receptor (nAChR) subunits, suggesting that the excitability of neurons in the IC can be altered by cholinergic signaling. However, the cellular-level mechanisms of cholinergic signaling in the IC remained unknown. In Chapter 2, I showed that VIP neurons in the IC are strongly modulated by ACh. By using whole-cell current clamp recording and pharmacology, I determined that the effect of ACh on VIP neurons is mediated by $\alpha_3\beta_4$* nAChRs. These results present the first, cellular-level mechanism for cholinergic modulation of a specific neuron type in the IC and provide fundamental knowledge for in vivo studies exploring the role of ACh signaling during auditory learning and processing.

The MG acts as the thalamic relay center of auditory information. It is a complex of nuclei that receives a combination of excitatory and inhibitory inputs from the IC. This region strongly expresses the receptors for the vasoactive intestinal peptide (VIP), a neuropeptide that can modulate intrinsic properties of neurons and even affect synaptic transmission. However, the effects of VIP on the excitability of MG neurons, and the sources of VIP signaling to the MG remained unknown. Recent studies showed that IC VIP neurons send direct projections to the MG. I hypothesized that IC VIP neurons provide direct VIP signaling to the MG, affecting the excitability of the neurons in the thalamus. By using electrophysiology, pharmacology, and in situ hybridization, I determined that VIP depolarizes MG neurons via the activation of VIP receptor 2 (VIPR2). Furthermore, by using retrograde tracing, I found that VIP neurons from both the IC and auditory cortex send long range projections to the MG, suggesting that the MG receives VIP signaling from different brain regions. These results provide the first evidence for VIP modulation in the MG and open the door to studying how differing neuromodulator sources affect the excitability of neurons during auditory processing.

Lastly, in Chapter 4 I summarize the findings presented in this dissertation and provide insight on future experiments and approaches to further our understanding of the role of neuromodulators in the auditory pathway.

Chapter 1 Introduction

1.1 Organization of the Central Auditory Pathway

The central auditory pathway is the neural circuit responsible for processing sound information in the brain (Winer & Schreiner, 2005). The pathway begins at the cochlea, a spiral-shaped organ in the inner ear, where sound waves are converted into electrical signals by specialized hair cells. From the cochlea, the signals are transmitted to the brainstem via the vestibulocochlear nerve. In the brainstem, the auditory signals are first processed by the cochlear nucleus, a group of nuclei that receives input from the ear and helps determine the location and timing of sounds. From there, signals travel to several auditory brain regions including the superior olivary complex, where binaural cues are processed to localize sound sources. Next, the signals pass through the inferior colliculus (IC), a structure located in the midbrain and considered the hub of the auditory pathway. In this region, auditory inputs converge to integrate information on the frequency and intensity of sounds, sound source locations, as well as vocalizations and speech cues. Furthermore, the IC is a major site for binaural integration due to both sides of the IC being connected via prominent commissural projections. The IC sends direct projections to the medial geniculate body (MG), the auditory thalamic nucleus. The MG acts as a relay station for sensory information, while filtering and sorting incoming signals by frequency and specific binaural properties before they reach the cortex. Finally, the signals are transmitted to the auditory cortex, a region of the brain located in the temporal lobe that is responsible for processing and interpreting sound information. Here, the signals are decoded and transformed into meaningful auditory perceptions such as speech, music, and environmental sounds.

Although the general anatomy of the central auditory system has been mapped thoroughly, many questions remain on how our brains identify and respond to auditory cues. It is imperative that we further understand the cellular mechanisms that govern auditory processing to expand our knowledge of hearing and sound processing. To address this gap in knowledge, here I studied the mechanisms governing the excitability of neurons of two subcortical auditory brain regions: the IC and the MG.

1.1.1 The inferior colliculus is important for sound processing.

The IC is a midbrain structure that plays a crucial role in the processing of auditory information. The IC is a tonotopically organized structure divided into three subdivisions, each receiving excitatory and inhibitory inputs from different sources (Adams, 1979; Brunso-Bechtold et al., 1981; Frisina et al., 1998; Saldaña et al., 1996; Winer et al., 1998). Neurons in the IC respond selectively to diverse sound features, such as frequency, intensity, and temporal pattern, and are sensitive to the spatial location of sound sources (Aitkin, 1991; Aitkin et al., 1994; Aitkin & Martin, 1987; Ehret & Merzenich, 1988; Syka et al., 2000). This brain structure is also a site for synaptic plasticity during hearing loss (Chambers et al., 2016). However, the cellular and local circuit mechanisms involved in sound processing in the IC have largely eluded the field due to lack of understanding of how incoming auditory cues affect the excitability of neurons.

1.1.2 The Medial Geniculate Body as an auditory processing and relay nucleus.

The MG acts as the thalamic relay center of auditory information. It is a complex of nuclei that receives a combination of excitatory and inhibitory inputs from the IC, reticular thalamic nucleus, and auditory cortex (Andersen et al., 1980; Calford & Aitkin, 1983; Jones, 1975; Jones & Rockel, 1971; Kudo & Niimi, 1978; Mellott et al., 2014; Montero, 1983; Rouiller

et al., 1985; Rouiller & de Ribaupierre, 1985). The MG subdivisions are known to be responsible for processing different auditory information, suggesting a functional role for each subdivision during auditory processing (Popper & Fay, 1992). Because of these characteristics, the MG might be more than a relay center, as it may process and therefore alter ascending auditory information before sending that information to the cortex. This hypothesis is further supported by data showing that neurons and presynaptic terminals in the MG express the receptors for non-glutamatergic and non-GABAergic signaling molecules (Fitzpatrick et al., 1989; Hill et al., 1992; Sottile et al., 2017). Therefore, the MG may be an important nucleus for auditory processing, where ascending and descending inputs converge and are modulated, leading to appropriate behavioral responses to sound cues.

1.2 Identifying neuron types in the inferior colliculus.

The neuronal populations in the IC have been studied with the goal of identifying distinct classes of neurons to further understand the cellular mechanisms, organization, and function of the IC. Early studies showed that IC neurons have stellate or disc-shaped morphologies (Malmierca et al., 1993; Oliver & Morest, 1984), express either the GABA or glutamate neurotransmitters, and have a spectrum of responses to auditory cues. However, none of these properties had conclusively identified a neuron class in the IC. Our lab recently found the first molecularly identifiable neuron type in the IC (Goyer et al., 2019), called VIP neurons. These neurons express mRNA for Vasoactive Intestinal Peptide (VIP), a 28 amino acid peptide known to be involved in regulatory mechanisms of the central and peripheral nervous systems (Gozes & Brenneman, 1989). VIP neurons in the IC are glutamatergic, have spiny dendrites and express N-methyl-D-aspartate receptors (NMDARs), cellular and molecular components important for synaptic plasticity. Our lab's previous work also found that VIP neurons send direct projections

within the IC, to the contralateral IC via the commissure, and to the superior olivary complex, the nucleus of the brachium of the IC, auditory thalamus, periaqueductal grey, and the superior colliculus. The expression of molecular components important for synaptic plasticity, as well as the broad projection pattern of IC VIP neurons suggest that this principal neuron type plays an important role in modulating auditory learning and behavioral responses by modulating the excitability of downstream targets via glutamatergic and neuropeptide signaling. The characterization of VIP neurons in the IC presents the opportunity to determine the cellular-level mechanisms of neuromodulation in a defined neuron class of IC neurons, which were previously unexplored due to the gap in knowledge about neuronal types in this region.

1.3 Neuromodulation is important for sensory processing.

Neuromodulators are neurotransmitters that can change the excitable state of a neuron via non-glutamatergic and non-GABAergic receptors (Ito & Schuman, 2008). Neuromodulators can affect the excitability of neurons by regulating processes such as neurotransmitter release from presynaptic terminals, the amplitude and kinetics of postsynaptic currents, regulating calcium influx, and regulating receptor expression via secondary messengers (Heckman et al., 2009; Higley & Sabatini, 2010; McKay et al., 2007; Rank et al., 2011; Regehr et al., 2009; Rosen et al., 1989; Sakurai et al., 2006). Neuromodulators can also act by regulating processes such as vasodilation, inflammation, stress regulation, and metabolism (Gozes & Brenneman, 1989; Kohlmeier & Reiner, 1999; Murphy et al., 1993; Wang et al., 1997). In this dissertation, I will discuss the roles and mechanisms of two neuromodulators commonly found in the brain: acetylcholine and vasoactive intestinal peptide.

1.3.1 Acetylcholine modulates the activity of neurons in the auditory pathway.

Acetylcholine (ACh) is a neurotransmitter that can change neuronal excitability, presynaptic release of neurotransmitters, and synchronize firing of groups of neurons in the brain (Kawai et al., 2007; Rice & Cragg, 2004; Wonnacott, 1997; Zhang & Sulzer, 2004). In cerebral cortex, it is known that nicotine increases neural responses in regions associated with attention and sensory processing (Disney et al., 2007; Sun et al., 2017). The pontomesencephalic tegmentum (PMT) provides extensive cholinergic inputs to different levels of the auditory system, including the IC and the MG (Motts & Schofield, 2009). PMT excitability is influenced by behavioral state, attention, and novel sensory experiences (Boucetta et al., 2014; Jones, 1991; Kozak et al., 2005; Schofield et al., 2011). Therefore, it is hypothesized that changes in the excitability of PMT cholinergic neurons in different behavioral states and contexts can directly influence auditory processing by modulating the excitability of downstream auditory targets via cholinergic neurotransmission. This hypothesis is further supported by studies that show strong expression of cholinergic receptors within the auditory pathway (Bieszczad et al., 2012; Clarke et al., 1985; Happe & Morley, 2004; Sottile et al., 2017; Wada et al., 1989). In the IC, in vivo studies determined that nicotine, an agonist of nicotinic acetylcholine receptors (nAChRs), affects the gain of input-output functions of neurons (Farley et al., 1983; Habbicht & Vater, 1996). Furthermore, nicotine induces changes in IC processing that may enhance auditory attention (Knott et al., 2012; Pham et al., 2020; Smucny et al., 2016).

Cholinergic signaling is also implicated in plasticity mechanism in the IC, where it has been shown that ACh signaling in awake bats leads to shifts in the best frequency of neurons (Ji et al., 2001). It is also known that during fear conditioning, ACh plays a role in augmenting the responses to tone bursts paired with leg shocks, suggesting a role for cholinergic modulation in different behavioral states (Ji et al., 2005). However, the role of ACh in neuromodulation and

plasticity mechanisms is less understood at the cellular level, sparking the need to understand the effect of ACh in specific neuron populations of the IC.

1.3.2 VIP signaling is a modulator of physiological processes.

VIP is involved in a variety of regulatory mechanisms of the central and peripheral nervous systems (Gozes & Brenneman, 1989). The effects of VIP have been studied in several parts of the central nervous system (CNS), with studies showing that VIP can modulate intrinsic properties of neurons and even affect synaptic transmission (Gozes & Brenneman, 1989; Kohlmeier & Reiner, 1999; Murphy et al., 1993; Wang et al., 1997). Based on these findings, it is predicted that VIP affects sensory processing. This hypothesis is supported by studies that show expression of VIP receptors (VIPRs) in thalamic relay nuclei (Sheward et al., 1995; Usdin et al., 1994; Vertongen et al., 1997), and evidence showing that VIP strongly excites neurons in somatosensory thalamus (Lee & Cox, 2003; Sun et al., 2003). The MG expresses VIPRs in all its subdivisions and has one of the highest levels of VIPRs in the brain (Hill et al., 1992). Despite the potential of VIP modulating the excitability of thalamocortical neurons in the MG during auditory processing, the role and source of VIP signaling to this region remain unexplored.

1.4 The effect of acetylcholine on VIP neuron excitability.

Physiological recordings paired with acoustic stimuli and cholinergic agonists and antagonists show that IC neurons are excited by ACh (Farley et al., 1983; Habbicht & Vater, 1996; Watanabe & Simada, 1973). In addition, nAChRs are expressed by many neurons throughout the IC (Schwartz, 1986; Sottile et al., 2017). However, the mechanisms that govern cholinergic neurotransmission and how these affect the excitability of specific neuron populations in the IC are still unknown. Askew et al. (2019) showed that activation of nAChRs

in cortical VIP neurons led to a prolonged depolarization. With these findings, along with the expression of nAChRs in the IC, I hypothesized that VIP neurons in the IC are affected by ACh via mechanisms that parallel those found in cortex. Elucidating the role of cholinergic neurotransmission in the IC will provide fundamental knowledge on the neuromodulatory mechanisms of synaptic plasticity and auditory learning in a subcortical brain region of the central auditory pathway.

1.5 The role and source of VIP signaling to the auditory thalamus remain unclear.

VIP is known to affect the excitability of neurons in the somatosensory thalamus via the activation of VIPRs (Lee & Cox, 2003; Sun et al., 2003). However, the role of VIP in the auditory thalamus remains unclear. Based on the effects of VIP in other thalamic nuclei, I hypothesized that VIP plays a role in affecting the excitability and intrinsic properties of MG neurons during auditory processing. This hypothesis is further supported by studies showing that the MG strongly expresses VIPRs (Hill et al., 1992). Despite the potential of VIP modulating the excitability of thalamocortical neurons in the MG during auditory processing, the role and source of VIP signaling to this region remain unexplored. With the identification of VIP neurons in the IC and their long-range projections to the MG (Goyer et al., 2019), I further examined the role of VIP signaling in the MG and the potential sources of VIP signaling to this region.

1.6 Summary and aims of dissertation.

Hearing loss, which affects more than 37.5 million adults in the United States, is a major factor contributing to cognitive decline and dementia (Lin et al., 2013). Recent research has focused on studying cholinergic neurotransmission as a mechanism to modulate the excitability of the auditory system and develop novel hearing loss treatments. However, fundamental

knowledge on the cellular mechanisms that govern cholinergic modulation in the IC remained largely unknown. With the IC receiving direct cholinergic inputs and being an important site of synaptic plasticity (Ji et al., 2001, 2005), it is surprising we know so little about how specific neuron populations in this region are affected by cholinergic modulation. The overall objective of this dissertation is to determine how cholinergic modulation influences the excitability of VIP neurons and their output to neurons in the MG. My central hypothesis is that ACh enhances the intrinsic excitability of VIP neurons in the IC through the activation of cholinergic receptors, leading to strong excitation of MG neurons through increased release of glutamate and VIP. To address this hypothesis, this dissertation is divided into two aims. The first aim focuses on studying the cellular-level mechanisms of ACh signaling in the IC. Previous research has broadly studied the effects of ACh on the activity of IC neurons, with little information provided on the neuron types and receptors involved in these excitability changes. Determining how ACh affects VIP neurons in the IC provides valuable information on the mechanisms of ACh-mediated synaptic plasticity in this region. The results of this aim will be discussed in Chapter 2, where a genetically modified mouse model was used to selectively target electrophysiological recordings to VIP neurons in the IC and elucidate the cholinergic effects on this specific neuron type. The second aim focuses on understanding the role of VIP signaling in the MG. Previous studies show the MG expresses receptors for VIP, but the effect of VIP and the sources of this neuropeptide to the MG remain unknown. The results in Chapter 3 provide insight on the role of VIP signaling in the MG, as well as the receptors and sources of signaling involved in this process. In Chapter 4 I discuss the significance of ACh and VIP neuromodulation in the auditory system, and propose future research directions to further our knowledge on the role of neuromodulators in the tectothalamic pathway of the auditory system.

Chapter 2 $\alpha_3\beta_4^*$ Nicotinic Acetylcholine Receptors Strongly Modulate the Excitability of VIP Neurons in the Mouse Inferior Colliculus

2.1 Introduction

Growing evidence indicates that cholinergic signaling through nicotinic acetylcholine receptors (nAChRs) critically shapes sound processing in the central auditory system (Askew et al., 2017; Felix et al., 2019; Goyer et al., 2016; Zhang et al., 2021). The inferior colliculus (IC), the midbrain hub of the central auditory system, receives extensive input from cholinergic neurons in the pontomesencephalic tegmentum (PMT; Motts and Schofield, 2009), and expresses several nAChR subunits, including α_3, α_4, α_7, β_2, β_3, and β_4 (Bieszczad et al., 2012; Clarke et al., 1985; Gahring et al., 2004; Happe & Morley, 2004; Morley & Happe, 2000; Salas et al., 2003; Sottile et al., 2017; Wada et al., 1989; Whiteaker et al., 2002). Because activity in the PMT is influenced by the sleep-wake cycle, attention, rewards, and sensory novelty, it is hypothesized that PMT neurons regulate auditory processing in the IC as a function of behavioral state (Boucetta et al., 2014; Jones, 1991; Kozak et al., 2005; Schofield et al., 2011). Consistent with this, in vivo studies have shown that nicotinic drugs alter the gain of input-output functions in IC neurons (Farley et al., 1983; Habbicht & Vater, 1996), and human psychophysics studies indicate that nicotine improves performance in auditory attention and discrimination tasks (Knott et al., 2012; Pham et al., 2020; Smucny et al., 2016), an effect partly attributable to alterations in the IC (Askew et al., 2017). In addition, temporal coding of auditory stimuli is degraded in the IC of α_7 knockout mice (Felix et al., 2019). However, despite the importance of nAChRs to auditory

processing, the cellular mechanisms by which nAChRs influence the excitability of IC neurons remain largely unknown.

This gap in knowledge has eluded the field mostly due to the complexity of the neuronal populations in the IC, where it has proven difficult to identify and study specific neuron classes using conventional approaches. We recently overcame this obstacle, identifying vasoactive intestinal peptide (VIP) neurons as the first molecularly identifiable neuron class in the IC (Goyer et al., 2019). Vasoactive intestinal peptide neurons are found throughout the major IC subdivisions, they are glutamatergic, and they have a stellate morphology with spiny dendrites that, within the central nucleus of the IC (ICc), typically extend across two or more isofrequency laminae. Vasoactive intestinal peptide neurons project to several auditory regions, including the auditory thalamus, superior olivary complex, and the contralateral IC, and they receive input from the dorsal cochlear nucleus, the contralateral IC, and likely from other sources. By using the VIP-IRES-Cre mouse model, we can selectively target VIP neurons for electrophysiological and anatomical experiments. Thus, we are in a position for the first time to determine the cellular mechanisms of cholinergic signaling in a defined class of IC neurons.

Here, we hypothesized that the excitability of VIP neurons in the IC is modulated by cholinergic signaling. Using immunofluorescence, we showed that cholinergic terminals are frequently located in close proximity to VIP neurons, suggesting that VIP neurons receive direct cholinergic input. We then found that brief applications of ACh elicited surprisingly long periods of depolarization and spiking in VIP neurons. These responses were not affected by atropine, a muscarinic acetylcholine receptor (mAChR) antagonist, but were largely blocked by mecamylamine, an antagonist partially selective for β_4-containing receptors, and by SR16584, an antagonist selective for $\alpha_3\beta_4$* receptors (* indicates that the identity of the fifth subunit in the

receptor pentamer is unknown). Consistent with this, voltage clamp recordings showed that ACh puffs led to prolonged inward currents that were largely blocked by mecamylamine and by SR16584. Moreover, cholinergic responses were resistant to manipulations affecting synaptic transmission, indicating that the nAChRs mediating these responses are expressed by VIP neurons. Finally, we showed that 10 and 30 Hz trains of lower concentration ACh puffs elicited temporal summation in VIP neurons, suggesting that the in vivo firing patterns of cholinergic PMT neurons are likely to drive prolonged excitation of VIP neurons. We thus provide the first evidence that $\alpha_3\beta_4$* nAChRs, a subtype with limited distribution in the brain, elicit direct and potent excitation of IC VIP neurons. Combined, our data reveal that cholinergic modulation exerts a surprisingly potent and long-lasting increase in the excitability of an important class of IC principal neurons.

2.2 Results

2.2.1 Cholinergic Synapses Are Found Adjacent to the Somas and Dendrites of VIP Neurons

The IC receives cholinergic input from the two nuclei that comprise the PMT: the pedunculopontine tegmental nucleus and the laterodorsal tegmental nucleus. Together, these nuclei distribute cholinergic axons and synapses throughout the IC, contacting both GABAergic and glutamatergic neurons (Beebe & Schofield, 2021; Motts & Schofield, 2009; Noftz et al., 2020; Schofield et al., 2011). However, the specific neuronal populations that cholinergic terminals synapse onto in the IC remain unclear. To test whether VIP neurons receive cholinergic input, we performed immunofluorescence on brain slices from VIP-IRES-Cre x Ai14 mice, in which VIP neurons express the fluorescent protein tdTomato, using an antibody against the vesicular acetylcholine transporter (VAChT). High resolution images were collected using a laser-scanning confocal microscope with a 1.40 NA 63x oil-immersion objective and 0.1 μm Z-

steps. Analysis of these images showed that VAChT+ boutons and terminals were routinely located <2 μm from the somas, dendrites, or both of VIP neurons (Figure 1). Similar results were observed in IC sections from five mice. These results suggest that VIP neurons receive cholinergic input (Rees et al., 2017). We therefore hypothesized that cholinergic signaling modulates the excitability of VIP neurons.

2.2.2 Brief Puffs of ACh Drive Prolonged Firing in VIP Neurons Via Non-α_7 nAChRs

To test whether acetylcholine alters the excitability of VIP neurons, we targeted current clamp recordings to fluorescent VIP neurons in acute IC slices from VIP-IRES-Cre x Ai14 mice and used a puffer pipette to provide brief puffs of ACh near the recorded cell. We found that 10 ms puffs of 1 mM ACh delivered approximately 20 μm from the VIP cell soma drove depolarization and firing in 116 out of 126 VIP neurons. These effects were surprisingly strong and long-lasting, suggesting that cholinergic signaling can potently increase the excitability of VIP neurons (Figure 2).

Since ACh depolarized VIP neurons for up to 1 s, we first hypothesized that this effect was mediated by a slow metabotropic mechanism involving mAChRs. However, we found that ACh-mediated excitation of VIP neurons was not altered by 1 μM atropine, a mAChR antagonist, indicating that mAChRs are not involved in this phenomenon (Figures 2A–C). For the remainder of this study, all recordings were conducted in the presence of 1 μM atropine, allowing us to isolate effects on nAChRs.

Next, we used mecamylamine (Mec), a broad-spectrum nAChR antagonist partially selective for β_4-containing nAChRs (Papke et al., 2008, 2010), and methyllycaconitine (MLA), an antagonist selective for α_7 nAChRs, to assess the contributions of nAChRs to the cholinergic excitation of VIP neurons. We found that bath application of 5 μM Mec nearly abolished the

firing and strongly reduced the depolarization elicited by ACh puffs on VIP neurons. When both 5 μM Mec and 5 nM MLA were applied, the remaining depolarization was nearly eliminated (Figures 2D–F). When 5 nM MLA was applied first, ACh-elicited firing and depolarization in VIP neurons were not significantly altered. Subsequent addition of 5 μM Mec to the bath abolished the ACh effect (Figures 2G–I). Combined, these results suggest that cholinergic modulation of VIP neurons is predominately driven by non-α_7, Mec-sensitive nAChRs.

2.2.3 Brief ACh Puffs Elicit a Long-Lasting Inward Current in VIP Neurons

nAChRs are commonly associated with fast, short-lasting depolarizations, but our data suggest that activation of nAChRs elicits prolonged depolarization in VIP neurons. To analyze the currents generated by activation of nAChRs in VIP neurons, we used voltage-clamp recordings with the holding potential at –60 mV. We found that a 10 ms puff of 1 mM ACh elicited an inward current in VIP neurons that lasted hundreds of milliseconds (mean decay τ = 438 ± 173 ms, mean ± SD, based on exponential fit; n = 5 neurons; Figure 3A). The peak of the ACh-evoked inward current was –329 ± 154 pA, and the 10 – 90% rise time was 89 ± 31 ms (mean ± SD, n = 5 neurons). Furthermore, similar to the depolarizations observed in our current-clamp experiments, 5 μM Mec abolished most of the current elicited by ACh, and the combination of 5 μM Mec and 5 nM MLA abolished the elicited current completely (Figure 3B). Therefore, our results suggest that the nAChRs mediating the effect of ACh on VIP neurons remain activated for extended periods, presumably due to slow kinetics and/or limited desensitization. Since α_7 nAChRs have fast kinetics and rapid desensitization (Anand et al., 1998; Castro & Albuquerque, 1993; Mike et al., 2000; Papke et al., 2000), both the pharmacology and kinetics of the inward currents observed here are consistent with a mechanism mediated by non-α_7 nAChRs.

2.2.4 ACh-Driven Firing in VIP Neurons Does Not Require Activation of Presynaptic nAChRs

Many glutamatergic and GABAergic neurons in the IC express nAChRs (Sottile et al., 2017). In addition, nAChRs are often located on presynaptic terminals where their activation can directly promote neurotransmitter release (Dani & Bertrand, 2007). Therefore, it is possible that the ACh-elicited excitation of VIP neurons requires activation of an intermediate population of neurons or terminals that in turn excite VIP neurons through the release of a different, non-cholinergic neurotransmitter. We therefore tested if cholinergic modulation of VIP neurons requires activation of receptors for glutamate, GABA, and/or glycine, the main neurotransmitters in the IC. By using pharmacology to block these receptors (10 μM NBQX to block AMPA receptors, 50 μM D-APV to block NMDA receptors, 5 μM gabazine to block $GABA_A$ receptors, and 1 μM strychnine to block glycine receptors), we isolated the effects of ACh puffs on VIP neurons from most other potential inputs. After bath application of the synaptic blockers, we observed that the spiking and depolarization elicited by ACh persisted and was not significantly altered (Figures 4A,B).

Next, we globally reduced synaptic release probability by decreasing the concentration of Ca^{2+} in the ACSF from 1.5 mM to 0.5 mM. Since the relationship between release probability and extracellular Ca^{2+} is described by a power law (Dodge & Rahamimoff, 1967), this reduction in ACSF Ca^{2+} should dramatically decrease neurotransmitter release. We observed that decreasing extracellular Ca^{2+} did not significantly alter the spiking or depolarization elicited by ACh puffs on VIP neurons (Figures 4C,D). These results suggest that ACh acts on nAChRs present on VIP neurons themselves, and not via activation of presynaptic nAChRs.

*2.2.5 $\alpha_4\beta_2$*nAChRs Do Not Mediate the Effect of ACh on VIP Neurons*

Our results thus far indicate that Mec-sensitive nAChRs mediate most of the effect of ACh on VIP neurons. However, Mec is a relatively broad-spectrum antagonist of non-homomeric nAChRs, with subtype selectivity depending on the concentration used (Papke et al., 2001, 2008, 2010). Since $\alpha_4\beta_2$* nAChRs are widely expressed in the IC and are the most common subtype of nAChR found in the brain (Millar & Gotti, 2009), we performed current-clamp recordings to assess how DHβE, a selective antagonist for $\alpha_4\beta_2$* nAChRs, affected the response of VIP neurons to ACh puffs. After bath-applying 10 μM DHβE for 10 min, our results showed that blocking $\alpha_4\beta_2$* nAChRs did not significantly alter the spiking or depolarization elicited by ACh application (Figure 5). Therefore, our data suggest that cholinergic modulation of VIP neurons involves little or no contribution from $\alpha_4\beta_2$* or α_7 nAChRs, the most common nAChRs in the brain.

*2.2.6 ACh-Driven Excitation of VIP Neurons Is Mediated by $\alpha_3\beta_4$*nAChRs*

Although $\alpha_3\beta_4$* nAChRs are relatively rare in the brain, previous studies indicate that α_3 and β_4 nAChR subunits are expressed in the IC (Gahring et al., 2004; Marks et al., 2002, 2006; Salas et al., 2003; Wada et al., 1989; Whiteaker et al., 2002). In addition, Mec strongly antagonizes $\alpha_3\beta_4$* nAChRs at a concentration of 5 μM (Papke et al., 2008, 2010), which we used in our current-clamp and voltage-clamp recordings. We therefore hypothesized that $\alpha_3\beta_4$* nAChRs mediate the excitatory effect of ACh on VIP neurons. To test this, we used SR16584, a selective $\alpha_3\beta_4$* nAChR antagonist (Zaveri et al., 2010). Because SR16584 is dissolved in DMSO, we first established that a vehicle control (1:1000 DMSO:ACSF) did not affect the ability of 10 ms puffs of 1 mM ACh to excite VIP neurons (Figures 6A–C). Next, we bath applied 50 μM SR16584 and found that it nearly abolished the spiking and strongly reduced the depolarization

elicited by ACh (Figures 6A–C), similar to our results with Mec applications. Furthermore, after only a 10-min washout of SR16584, the excitatory effect of ACh partially recovered.

2.2.7 ACh-Induced Inward Currents in VIP Neurons Are Predominately Mediated by $\alpha_3\beta_4$ nAChRs*

Based on our current-clamp results, we hypothesized that bath application of SR16584 would abolish most of the inward current elicited by ACh in VIP neurons. To test this, we performed voltage-clamp recordings as described above. As before, ACh elicited large and sustained inward currents that were not altered by the vehicle control (Figure 6D). Application of 50 μM SR16584 abolished 93 ± 6% of the inward current on average (mean ± SD), revealing a much smaller and faster current in 6 of 7 recorded cells, similar to that observed during application of Mec. This remaining current was blocked by application of 5 nM MLA plus 50 μM SR16584, suggesting that it was mediated by α_7 nAChRs (Figures 6D,E). Together with our current clamp results, these results demonstrate that ACh-induced excitation of VIP neurons is mediated mainly by $\alpha_3\beta_4$* nAChRs and provide the first evidence for a functional role of $\alpha_3\beta_4$* nAChRs in the IC.

2.2.8 Repeated ACh Pulses Elicit Temporal Summation in VIP Neurons

Thus far we have examined how isolated puffs of 1 mM ACh affected the excitability of VIP neurons. However, the time course and concentration of ACh released from cholinergic synapses onto VIP neurons in vivo is unknown. Previous studies show that the average firing rates of cholinergic PMT neurons in vivo tend to be rather low, typically less than a few Hz (Boucetta et al., 2014), but arousing sensory stimuli elicit brief bursts of firing that can reach 100 – 200 Hz (Reese et al., 1995a, 1995b; Sakai, 2012). In addition, our immunofluorescence data

suggest that VIP neurons often receive multiple cholinergic inputs, which may reflect convergence from multiple PMT neurons. We therefore decided to test the effects of 10 and 30 Hz trains of ACh puffs, reasoning that VIP neurons would likely encounter these frequencies of input in vivo. Based on the slow kinetics and limited desensitization of $\alpha_3\beta_4$* nAChRs (David et al., 2010), we hypothesized that lower concentrations of ACh delivered in trains would elicit long-lasting excitation of VIP neurons due to temporal summation of cholinergic EPSPs. To test this, we made current-clamp recordings from VIP neurons while delivering trains of 1 – 10 puffs of 30 μM or 100 μM ACh at 10 Hz (Figures 7A,E) or 30 μM ACh at 30 Hz (Figure 7I). We observed that as the number of puffs increased, VIP neurons increasingly depolarized and could transition from firing no spikes in response to a single ACh puff to firing trains of spikes in response multiple ACh puffs (Figures 7B,F,J). The amount of depolarization elicited by increasing numbers of ACh puffs, as measured by the average area under the median-filtered trace, produced rising input-output functions (Figures 7C,G,K). Linear fits to the means of the normalized responses for 10 Hz trains had slopes of 1.4 and 4.0 normalized units/puff, indicating that temporal summation was supralinear on average for both 30 μM and 100 μM puff trains, respectively (cyan data, Figures 7D,H). The 30 Hz trains of 30 μM ACh puffs resulted in sublinear integration, with a linear fit to the means of the normalized responses having a slope of 0.38 normalized units/puff (cyan data, Figure 7L). Although this relationship was sublinear, the slope was positive, and temporal summation still occurred, with the total depolarization after 10 puffs being 3.8x that elicited by a single puff.

Together, these results suggest that even if cholinergic synapses in vivo elicit smaller and/or briefer EPSPs, these EPSPs will be subject to temporal summation during periods of heightened PMT activity, thereby driving excitation of VIP neurons more effectively than

isolated inputs. In addition, our results point to a potentially complicated relationship between the frequency of cholinergic input trains and the extent of temporal summation, suggesting that different patterns of cholinergic input may support diverse computations in VIP neurons. A more comprehensive analysis of the relationship between cholinergic input frequency and temporal summation in VIP neurons awaits a future study when cholinergic inputs to VIP neurons can be directly stimulated, most likely with optogenetics, over a wider range of frequencies. The present results suggest that specific patterns of cholinergic excitation can combine in diverse ways with the ascending and local auditory inputs that VIP neurons receive (Goyer et al., 2019) to critically reshape auditory processing in VIP neurons and their postsynaptic targets.

2.3 Discussion

Here, we report the first cellular-level mechanism for cholinergic modulation in the auditory midbrain. Our data show that cholinergic terminals are routinely found in close proximity to the dendrites and somas of VIP neurons in the IC. In whole-cell recordings, brief applications of ACh to VIP neurons elicited surprisingly strong, long-lasting depolarizations and sustained inward currents. Despite the prolonged nature of these responses, they were not altered by blocking muscarinic receptors. Instead, using several nAChR antagonists, we determined that ACh excites VIP neurons mainly by activating $\alpha_3\beta_4$* nAChRs, with a small contribution from α_7 nAChRs. $\alpha_3\beta_4$* nAChRs are rare in the brain and have mainly been studied in the medial habenula and interpeduncular nucleus, where they play an important role in nicotine addiction (Beiranvand et al., 2014; Grady et al., 2009; Scholze et al., 2012; Sheffield et al., 2000). Our results uncover a novel role for $\alpha_3\beta_4$* receptors in the central auditory pathway, revealing a potent neuromodulatory mechanism in which ACh can drive a sustained increase in the excitability of VIP neurons. Since VIP neurons project locally, to the auditory thalamus, and to

several other auditory and non-auditory brain regions, cholinergic modulation of VIP neurons has the potential to exert widespread influence on auditory processing and its downstream effects.

*2.3.1 $\alpha_3\beta_4$*nAChRs Mediate Prolonged Depolarization of VIP Neurons*

Although nAChRs are often noted for driving fast and brief responses to cholinergic inputs, these effects are generally attributable to α_7 nAChRs, which have fast kinetics and rapid desensitization (Arroyo et al., 2012; Bennett et al., 2012; Christophe et al., 2002). A growing number of studies have documented instances in which non-α_7 nAChRs mediate longer-lasting changes in neuronal excitability. For example, in VIP interneurons in the auditory cortex, nicotine induces firing for up to several minutes, and this effect was blocked by DHβE, an $\alpha_4\beta_2$* nAChR antagonist (Askew et al., 2019). In layer 1 of cerebral cortex, α_7 nAChRs mediate an early, fast response to ACh, while non-α_7 nAChRs mediate a later, slower response (Arroyo et al., 2012; Bennett et al., 2012; Christophe et al., 2002). Likewise, at the motoneuron-Renshaw cell synapse in the spinal cord, in combination with glutamatergic signaling, homomeric α_7 nAChRs mediate an early, fast response to ACh, while $\alpha_4\beta_2$* nAChRs mediate a slower, longer-lasting response (d'Incamps et al., 2012; Lamotte d'Incamps et al., 2018; Lamotte d'Incamps & Ascher, 2008).

While previous studies show that mRNA for α_7, α_4, and β_2 nAChR subunits is common in the IC (Bieszczad et al., 2012; Clarke et al., 1985; Happe & Morley, 2004; Morley & Happe, 2000; Sottile et al., 2017; Wada et al., 1989), our data point to a limited role for α_7 and no functional role for $\alpha_4\beta_2$* nAChRs in VIP neurons. Instead, we found that $\alpha_3\beta_4$* nAChRs are the dominant nAChRs in VIP neurons, mediating a strong, long-lasting depolarization in response to ACh application. Consistent with our observations, $\alpha_3\beta_4$* nAChRs are capable of mediating

sustained currents due to their slow desensitization, with time constants on the order of seconds, and relatively long single-channel open times and burst durations (David et al., 2010). In addition, in situ hybridization studies and binding studies have consistently shown that the IC is one of the few places in the brain where α_3 and β_4 nAChRs are expressed (Gahring et al., 2004; Marks et al., 2002, 2006; Salas et al., 2003; Wada et al., 1989; Whiteaker et al., 2002), and β_4 knockout mice exhibit decreased α_3 mRNA levels in the IC, supporting the hypothesis that α_3 and β_4 subunits interact in the IC (Salas et al., 2004). Our findings confirm and extend these results by providing the first evidence of a functional role for $\alpha_3\beta_4$* nAChRs in the IC. Moreover, the widespread expression of α_3 and β_4 mRNA observed in past in situ hybridization studies suggests that other IC neuron types, in addition to VIP neurons, are likely to express $\alpha_3\beta_4$* nAChRs. Application of the pharmacological approach used here to additional neuron types will help expand our understanding of the functional roles of $\alpha_3\beta_4$* nAChRs in the IC.

It is important to note that $\alpha_3\beta_4$* nAChRs can have two stoichiometries, $(\alpha_3\beta_4)2\alpha_3$ or $(\alpha_3\beta_4)2\beta_4$, and can also combine with a different fifth subunit, $(\alpha_3\beta_4)2X$, where the fifth subunit can be α_2, α_5, α_6, or β_3 (Scholze & Huck, 2020). Previous studies indicate that the exact subunit composition of an $\alpha_3\beta_4$* nAChR has some effect on Ca^{2+} permeability and desensitization rate, but generally little or no effect on the potency and efficacy of ACh (Gerzanich et al., 1998; Groot-Kormelink et al., 2001; Papke et al., 2010; Stokes & Papke, 2012; Wang et al., 1996). It will be important for future studies to determine which type or types of $\alpha_3\beta_4$* nAChRs are expressed in VIP neurons.

2.3.2 Trains of Cholinergic Inputs May Drive Long-Lasting Modulatory Effects

To mimic more in vivo-like patterns of cholinergic input, we tested how VIP neurons responded to trains of ACh puffs. Our results show that, even at a relatively low application rate

of 10 Hz, cholinergic EPSPs underwent substantial temporal summation in VIP neurons. This temporal summation allowed 10 and 30 Hz trains of 30 μM ACh puffs to transition from eliciting no spikes with 1 or 3 puffs to multiple spikes with 5 or 10 puffs. Trains of 100 μM ACh puffs elicited an even more pronounced increase in firing. Although ACh puffs probably do not match the concentration and time course of synaptically released ACh in vivo, our results show that ACh strongly excited VIP neurons under a range of conditions, uncovering a cellular mechanism that likely drives similar effects in vivo and highlighting the need for future experiments to build on these results.

It is well established that cholinergic PMT neurons, the source of cholinergic input to the IC, alter their firing rate as a function of behavioral state. For example, Boucetta et al. found that cholinergic PMT neurons fired maximally during the active wake and paradoxical sleep states (mean firing rates of 2.3 Hz and 3.7 Hz, respectively) and nearly ceased firing during slow wave sleep (0.04 Hz) (Boucetta et al., 2014). Sakai found similar changes across the sleep-wake cycle, but also found that arousing stimuli (a hand clap or an air puff) drove cholinergic PMT neurons to fire bursts of 2 – 5 spikes with instantaneous frequencies of 100 – 200 Hz (Sakai, 2012). Many PMT neurons also respond to sensory stimuli. For example, almost half of PMT neurons fire in response to auditory click stimuli, with half of these neurons firing short latency bursts (Reese et al., 1995a, 1995b). Such responses might be driven by the primary auditory cortex, which projects to the PMT (Schofield, 2010; Schofield & Motts, 2009). Furthermore, our immunofluorescence data suggest that VIP neurons often integrate multiple cholinergic inputs. It therefore seems likely that certain behavioral states and sensory stimuli drive cholinergic input to VIP neurons at rates sufficient to elicit the temporal summation we observed. Thus, our data support the hypothesis that cholinergic input from the PMT drives prolonged increases in the

excitability in VIP neurons as a function of behavioral state and sensory input. Since VIP neurons project broadly within and beyond the IC, changes that alter cholinergic input to VIP neurons have the potential to drive wide-ranging changes in the excitability of the auditory and non-auditory circuits that VIP neurons target.

2.3.3 Functional Implications for Auditory Processing

Previous studies have identified clear roles for muscarinic signaling in the IC, including roles in cortically driven plasticity (Ji et al., 2001; Ji & Suga, 2009) and stimulus specific adaptation (Ayala & Malmierca, 2015), but the roles of nicotinic signaling in the IC are less clear. Psychophysical studies indicate that systemic nicotine exposure in non-smokers can enhance performance in auditory tasks (Harkrider & Hedrick, 2005; Knott et al., 2009; Pham et al., 2020). Intriguingly, recent work from Askew and colleagues suggests that systemic nicotine sharpens frequency tuning in the IC, which likely contributes to sharper tuning in auditory cortex and improved discrimination in behavioral tasks (Askew et al., 2017). However, the authors found that nicotine mainly suppressed activity in the IC. Since we found that activation of nAChRs increases VIP neuron excitability, this raises the interesting possibility that the local projections of VIP neurons might mainly target inhibitory neurons. Alternatively, a more complicated circuit interaction might occur. We plan to test how cholinergic modulation of VIP neurons shapes the auditory response properties of VIP neurons and their postsynaptic targets in future studies.

Finally, it is unknown how cholinergic signaling shapes the excitability of other IC neuron classes. The IC contains a rich diversity of neurons, but these have long proved difficult to reliably classify, making it difficult to investigate cholinergic modulation in a systematic way. Fortunately, in addition to VIP neurons, recent studies have identified GABAergic NPY neurons

(Silveira et al., 2020) and glutamatergic CCK neurons (Kreeger et al., 2021) as distinct IC neuron classes. To gain a fuller understanding of how cholinergic modulation shapes auditory processing in the IC, it will be important to determine the diverse effects cholinergic modulation exerts on these and other, yet to be identified, neuron classes.

2.4 Methods

2.4.1 Animals

All experiments were approved by the University of Michigan Institutional Animal Care and Use Committee and were in accordance with NIH guidelines for the care and use of laboratory animals. Animals were kept on a 12-h day/night cycle with ad libitum access to food and water. VIP-IRES-Cre mice ($Vip^{tm1(cre)Zjh}$/J, Jackson Laboratory, stock # 010908) (Taniguchi et al., 2011) were crossed with Ai14 reporter mice (B6.Cg-Gt(ROSA)26$Sor^{tm14(CAG–tdTomato)Hze}$/J, Jackson Laboratory, stock #007914) (Madisen et al., 2010) to yield F1 offspring that expressed the fluorescent protein tdTomato in VIP neurons. Because mice on the C57BL/6J background undergo age-related hearing loss, experiments were restricted to mice aged P30 – P85, an age range where hearing loss should be minimal or not present (Zheng et al., 1999).

2.4.2 Immunofluorescence

Mice aged P53 – P85 were deeply anesthetized with isoflurane and perfused transcardially with 0.1 M phosphate-buffered saline (PBS), pH 7.4, for 1 min and then with a 10% buffered formalin solution (Millipore Sigma, cat# HT501128) for 15 min. Brains were collected and post-fixed in the same formalin solution and cryoprotected overnight at 4°C in 0.1 M PBS containing 20% sucrose. Brains were cut into 40 µm sections on a vibratome. Sections were rinsed in 0.1 M PBS, and then treated with 10% normal donkey serum (Jackson

ImmunoResearch Laboratories, West Grove, PA) and 0.3% TritonX-100 for 2 h. Slices were incubated overnight at 4°C in rabbit anti-VAChT (3:500, Synaptic Systems, cat# 139103, RRID:AB_887864). This antibody was previously validated by Western blot and has been successfully used to identify cholinergic terminals in the cochlear nucleus and hippocampus (Gillet et al., 2018; Goyer et al., 2016; Zhang et al., 2019). The next day, sections were rinsed in 0.1 M PBS and incubated in Alexa Fluor 647-tagged donkey anti-rabbit IgG (1:500, ThermoFisher, cat# A-31573) for 2 h at room temperature. Sections were then mounted on slides (SouthernBiotech, cat# SLD01-BX) and coverslipped using Fluoromount-G (SouthernBiotech, cat# 0100–01). Images were collected using a 1.40 NA 63x oil-immersion objective and 0.1 μm Z-steps on a Leica TCS SP8 laser scanning confocal microscope.

2.4.3 Analysis of Cholinergic Terminals Adjacent to VIP Neurons

After immunofluorescence was performed, we used Neurolucida 360 software (MBF Bioscience) to reconstruct VIP neurons and assess the distribution of cholinergic terminals on reconstructed neurons. Terminals that were <2 μm from the dendrites or soma of the reconstructed cell were counted as synapses onto that neuron.

2.4.4 Brain Slice Preparation

Whole-cell patch-clamp recordings were performed in acutely prepared brain slices from VIP-IRES-Cre x Ai14 mice. Both males (n = 40) and females (n = 31) aged P30-P50 were used. No differences were observed between animals of different sexes. Mice were deeply anesthetized with isoflurane and then rapidly decapitated. The brain was removed, and a tissue block containing the IC was dissected in 34°C ACSF containing the following (in mM): 125 NaCl, 12.5 glucose, 25 $NaHCO_3$, 3 KCl, 1.25 NaH_2PO_4, 1.5 $CaCl_2$ and 1 $MgSO_4$, bubbled to a pH of

7.4 with 5% CO_2 in 95% O_2. Coronal sections of the IC (200 μm) were cut in 34°C ACSF with a vibrating microtome (VT1200S, Leica Biosystems) and incubated at 34°C for 30 min in ACSF bubbled with 5% CO_2 in 95% O_2. Slices were then incubated at room temperature for at least 30 min before being transferred to the recording chamber. All recordings were targeted at VIP neurons located in the central nucleus of the IC. Because the borders of IC subdivisions are not well-defined in acutely prepared slices, it is possible that a small number of VIP neurons were recorded from just outside the central nucleus, in the dorsal or lateral cortices of the IC.

2.4.5 Current-Clamp Electrophysiology

Slices were placed in a recording chamber under a fixed stage upright microscope (BX51WI, Olympus Life Sciences) and were constantly perfused with 34°C ACSF at ~2 ml/min. All recordings were conducted near physiological temperature (34°C). IC neurons were patched under visual control using epifluorescence and Dodt gradient-contrast imaging. Current-clamp recordings were performed with a BVC-700A patch clamp amplifier (Dagan Corporation). Data were low pass filtered at 10 kHz, sampled at 50 kHz with a National Instruments PCIe-6343 data acquisition board, and acquired using custom written algorithms in Igor Pro. Electrodes were pulled from borosilicate glass (outer diameter 1.5 mm, inner diameter 0.86 mm, Sutter Instrument) to a resistance of 3.5 – 5.0 MΩ using a P-1000 microelectrode puller (Sutter Instrument). The electrode internal solution contained (in mM): 115 Kgluconate, 7.73 KCl, 0.5 EGTA, 10 HEPES, 10 Na_2 phosphocreatine, 4 MgATP, 0.3 NaGTP, supplemented with 0.1% biocytin (w/v), pH adjusted to 7.4 with KOH and osmolality to 290 mmol/kg with sucrose. Data were corrected for an 11 mV liquid junction potential.

To test the effect of ACh on the excitability of VIP neurons, acetylcholine chloride (Sigma cat # A6625), was freshly dissolved each day in a vehicle solution containing (in mM): 125 NaCl, 3 KCl, 12.5 Glucose and 3 HEPES. The solution was balanced to a pH of 7.40 with NaOH. The working concentration of ACh was 1 mM unless stated otherwise. To apply ACh puffs on brain slices, ACh solution was placed in pipettes pulled from borosilicate glass (outer diameter 1.5 mm, inner diameter 0.86 mm, Sutter Instrument) with a resistance of 3.5 – 5.0 MΩ using a P-1000 microelectrode puller (Sutter Instrument) connected to a pressure ejection system built based on the OpenSpritzer design (Forman et al., 2017). The puffer pipette was placed ~ 20 μm from the soma of the patched cell, and five 10 ms puff applications at 10 psi and 1 min apart were presented per condition. To isolate the receptors mediating the effects of ACh on VIP neurons, we bath applied the following drugs individually or in combination: 1 μM atropine (mAChR antagonist, Sigma), 5 μM mecamylamine (Mec, relatively non-selective antagonist with higher affinity for β_4 containing receptors, Sigma), 10 μM DHβE ($\alpha_4\beta_2$* nAChR antagonist, Tocris), 50 μM SR16584 ($\alpha_3\beta_4$* nAChR antagonist, Tocris), and 5 nM methyllycaconitine (MLA, α_7 nAChR antagonist, Sigma). All drugs were washed-in for 10 min before testing how the drugs affected the responses of the recorded neurons to ACh puffs. In one experiment, antagonists for $GABA_A$, glycine, AMPA, and NMDA receptors were bath applied to isolate direct effects of ACh on VIP neurons from possible ACh-induced changes in release from terminals synapsing onto VIP neurons. The following drug concentrations were used: 5 μM SR95531 (gabazine, $GABA_A$ receptor antagonist, Hello Bio), 1 μM strychnine hydrochloride (glycine receptor antagonist, Millipore Sigma), 10 μM NBQX disodium salt (AMPA receptor antagonist, Hello Bio), 50 μM D-AP5 (NMDA receptor antagonist, Hello Bio). All drugs were washed-in for 10 min before testing how the drugs affected the responses of the recorded

neurons to ACh puffs. Except for when the effects of atropine alone were directly tested, 1 μM atropine was included in the ACSF under all conditions.

2.4.6 Effect of Repeated ACh Applications

ACh puffs were applied as described above except at lower concentrations (30 μM and 100 μM). Trials containing trains of 1, 2, 3, 5, or 10 puffs at 10 Hz were delivered with a 1-min intertrial period. Five trials were presented per condition.

2.4.7 Voltage-Clamp Recordings of nAChR Currents

For voltage-clamp experiments, the recording setup was the same as above except that recordings were performed using an Axopatch 200A amplifier. During the recordings, series resistance compensation was performed using 90% prediction and 90% correction. The series resistance of the electrode was never greater than 10 MΩ. The electrode internal solution contained (in mM): 115 CsOH, 115 D-gluconic acid, 7.76 CsCl, 0.5 EGTA, 10 HEPES, 10 Na_2 phosphocreatine, 4 MgATP, 0.3 NaGTP, supplemented with 0.1% biocytin (w/v), pH adjusted to 7.4 with CsOH and osmolality to 290 mmol/kg with sucrose. As detailed above, the ACh puffer was placed approximately 20 μm from the soma of the patched cell, and five 10 ms puff applications at 10 psi were presented per condition, waiting 1 min between puffs. Receptor antagonists were applied as described above for the current clamp experiments. 1 μM atropine was included in the ACSF under all conditions. Voltage-clamp holding potentials were not corrected for the liquid junction potential.

2.4.8 Analysis of Electrophysiological Recordings

Action potential counts and measurements of the area under current clamp depolarizations and voltage clamp currents were made using custom written algorithms in Igor

Pro 8 (Wavemetrics). Action potential counts were made with a threshold-crossing algorithm and were verified by eye. To determine the area under current clamp depolarizations, data were first median filtered using a 4000 sample (80 ms) smoothing window to remove action potentials while leaving the waveform of the underlying slow depolarization intact. The area under the median-filtered depolarization was then calculated using the "Area" function. The area under voltage clamp currents was determined by applying the "Area" function to traces that were first median filtered using the same parameters as above. Responses to the five ACh puffs delivered per neuron per treatment condition were averaged, and these average values were used for the summary analyses.

2.4.9 Statistical Analyses

Data were analyzed and are presented following the estimation statistics approach, which emphasizes effect sizes and their confidence intervals over *p* values (Bernard, 2019; Calin-Jageman & Cumming, 2019). Results from null hypothesis significance tests are also provided, but a focus on the estimation statistics is encouraged. Data analysis and significance tests were performed using custom algorithms combined with the statistical functions available in Igor Pro 8 (Wavemetrics), MATLAB R2021a (MathWorks), and R 4.1.0 (The R Project for Statistical Computing).

In Figures 2–6, comparisons of results are shown using Gardner-Altman estimation plots (two groups) or Cumming estimation plots (three or more groups). The design of these plots was heavily influenced by the DABEST package (Ho et al., 2019), although the plots shown here were made using our own algorithms in MATLAB. Since our data involved repeated measures from individual cells, our estimation plots use parallel coordinates plots to show the measured responses for each cell, with each line representing data from one cell. The parallel coordinates

plots are accompanied by paired mean difference plots that show the pairwise differences between control responses and treatment responses. Paired mean differences are presented with bias-corrected and accelerated 95% bootstrap confidence intervals, which were generated using the "boot" package in R using 10,000 resampling iterations (Davison & Hinkley, 1997; Canty and Ripley, 2021). Bootstrap sampling distributions are plotted alongside the mean differences as histograms that were smoothed with the normal kernel function using the MATLAB "fitdist" command.

Statistical tests for differences between two groups were made using the "independence_test" function in the "coin" package in R (Hothorn et al., 2006, 2008). The "independence_test" is a non-parametric permutation test based on the theoretical framework of Strasser and Weber (Strasser & Weber, 1999). The "independence_test" was set to use a block design to represent the paired measurements in our data, to perform a two-sided test where the null hypothesis was zero Pearson correlation, and to generate the conditional null distribution using Monte Carlo resampling with 10,000 iterations. Statistical testing for differences between the control group and two or more treatment groups were made using linear mixed models (LMMs) implemented through the "lme4" and "lmerTest" packages in R (Bates et al., 2015; Kuznetsova et al., 2017). Drug treatments were the fixed effects and individual cells were the random effects. F statistics, t statistics, and p values for LMMs were generated using Satterthwaite's degrees of freedom method as implemented in the "lmerTest" package. In Figure 7, summary data for the responses to trains of acetylcholine puffs are presented as mean ± SD, and the summary data were fit with a linear regression performed in Igor Pro. Test statistics for all significance tests are reported in the figure legends. Effects were considered significant when $p < 0.05$.

2.5 Figures

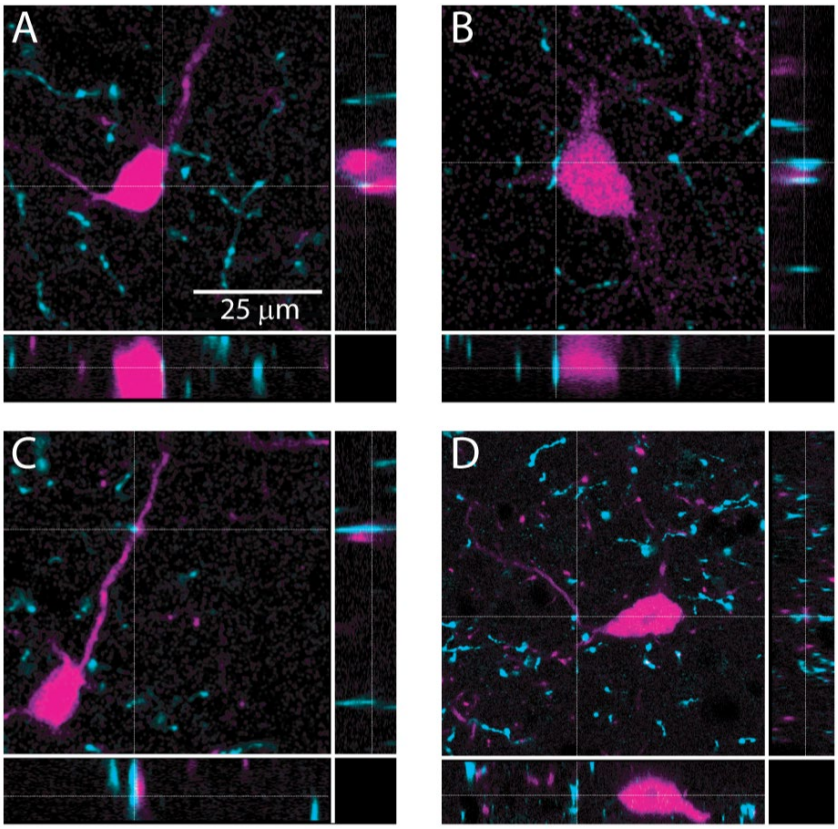

Figure 2-1 Cholinergic terminals are routinely found in close proximity to VIP neuron somas and dendrites.

Confocal images from IC sections show examples of cholinergic terminals (identified by dashed crosshairs) labeled by anti-VAChT (cyan) located <2 µm from the somas (top row, A,B) or dendrites (bottom row, C,D) of VIP neurons (magenta). The three panels in each image provide a top view and two side views centered on the cholinergic terminal identified by the crosshairs. Images are from 3 mice.

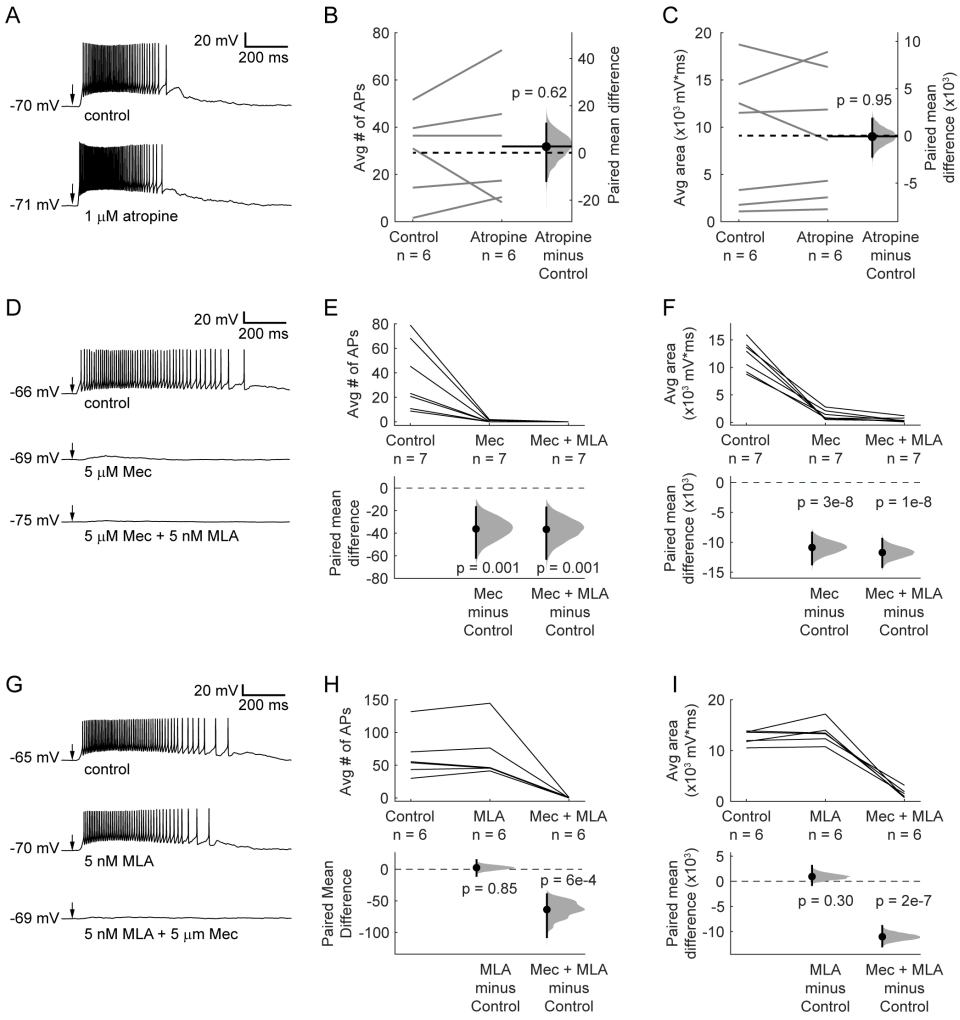

Figure 2-2 ACh-induced depolarization of VIP neurons is mediated by non-α_7 nAChRs.

A 10 ms puff of 1 mM ACh elicited a long-lasting depolarization and spiking in a representative VIP neuron under control conditions (top). 1 μM atropine did not alter the ACh response (bottom). (B,C) Atropine did not change the average number of action potentials elicited by ACh or the average area under the median-filtered curve (spikes: paired independence test, $Z = –0.486$, $p = 0.62$, $n = 6$; area: paired independence test, $Z = 0.086$, $p = 0.95$, $n = 6$). Dashed horizontal lines show the mean of the control responses. Solid horizontal lines show the mean difference between the control and atropine conditions. Note that in all remaining experiments, 1 μM atropine was always present in the ACSF. (D) Example traces show ACh-elicited depolarization in a VIP neuron in control ACSF (top), 5 μM Mec (middle), and 5 μM Mec + 5 nM MLA (bottom). (E) Mec reduced the average number of action potentials elicited by ACh puffs from 36.6 ± 28.2 to 0.4 ± 0.7 (mean ± SD; LMM: treatment effect, $F_{2,12} = 11.99$, $p = 0.001$, $n = 7$; control vs. Mec, $t_{12} = –4.22$, $p = 0.001$; control vs. Mec + MLA, $t_{12} = –4.26$, $p = 0.001$). (F) The total depolarization elicited by ACh puffs, measured as the area under the median filtered curve, was significantly decreased by Mec and further decreased by MLA (LMM: treatment effect $F_{2,12} = 111.6$, $p = 2e\text{-}8$, $n = 7$; control vs. Mec, $t_{12} = –12.43$, $p = 3e\text{-}8$; control vs. Mec + MLA, $t_{12} = –13.39$, $p = 1e\text{-}8$). (G) When MLA was applied before Mec, MLA alone did not have a clear effect on ACh responses. From top to bottom: control, 5 nM MLA, and 5 μM Mec + 5 nM MLA. (H) The average number of action potentials elicited by ACh was not significantly affected by MLA, while subsequent application of Mec + MLA eliminated firing (LMM: treatment effect, $F_{2,10} = 17.23$, $p = 6e\text{-}4$, $n = 6$; control vs. MLA, $t_{10} = 0.20$, $p = 0.85$; control vs. Mec + MLA, $t_{10} = –4.98$, $p = 6e\text{-}4$). (I) MLA alone did not significantly alter the depolarization elicited by ACh, while subsequent application of Mec + MLA caused an 89%

reduction in the average depolarization (LMM: treatment effect, $F_{2,10} = 120.4$, $p = 1e\text{-}7$, $n = 6$; control vs. MLA, $t_{10} = 1.10$, $p = 0.30$; control vs. Mec + MLA, $t_{10} = -12.85$, $p = 2e\text{-}7$). In (A,D,G) arrows indicate the time of the ACh puffs, and voltages indicate resting membrane potential. In (E,F,H,I), horizontal dashed lines indicate the level of zero mean difference, and vertical lines on the paired mean difference points indicate 95% bootstrap confidence intervals.

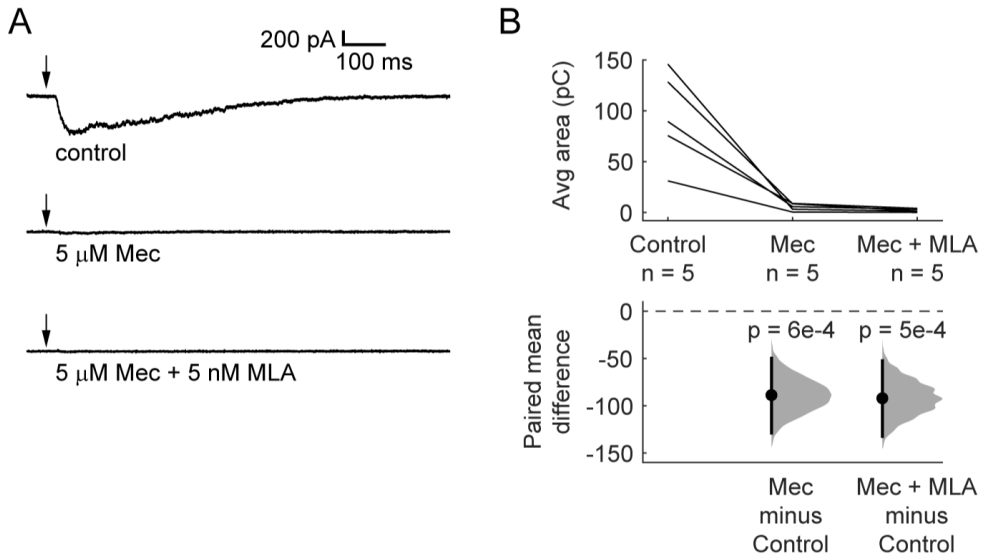

Figure 2-3 Brief ACh puffs elicit long-lasting inward currents in VIP neurons.

(A) Example traces of currents elicited by ACh puffs in control ACSF (top), 5 μM Mec (middle), and 5 μM Mec + 5 nM MLA (bottom). Arrows indicate the time of the ACh puffs. (B) The total charge flux elicited by ACh, measured by the average area under the median-filtered curve, significantly decreased after bath application of Mec. Subsequent application of MLA did not cause a further reduction (LMM: treatment effect, $F_{2,8} = 20.52$, $p = 7e\text{-}4$, $n = 5$; control vs. Mec, $t_8 = –5.44$, $p = 6e\text{-}4$; control vs. Mec + MLA, $t_8 = –5.65$, $p = 5e\text{-}4$). Horizontal dashed line indicates the level of zero mean difference. Vertical lines on the paired mean difference points indicate 95% bootstrap confidence intervals.

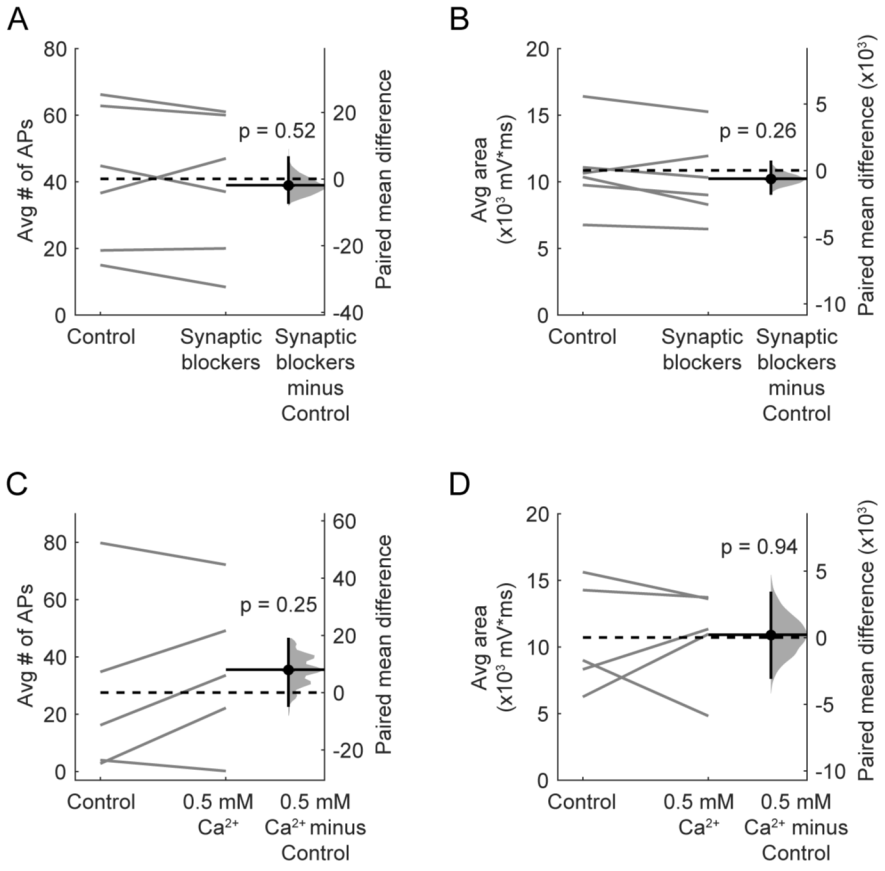

Figure 2-4 Depolarization of VIP neurons by ACh is consistent with an intrinsic mechanism and not presynaptic effects.

(A,B) The average number of action potentials (A) and depolarization (B) elicited by an ACh puff were not affected by bath application of antagonists against AMPA, NMDA, $GABA_A$, and glycine receptors (10 μM NBQX, 50 μM D-AP5, 5 μM SR95537, and 1 μM strychnine; action potentials: paired independence test, $Z = 0.724$, $p = 0.52$, $n = 6$; area: paired independence test, $Z = 1.28$, $p = 0.26$, $n = 6$). (C,D) The average number of action potentials (C) and depolarization (D) elicited by an ACh puff were unaffected by decreasing the ACSF Ca^{2+} concentration from 1.5 to 0.5 mM (action potentials: paired independence test, $Z = –1.29$, $p = 0.25$, $n = 5$; area: paired independence test, $Z = –0.137$, $p = 0.94$, $n = 5$). (A–D) Dashed horizontal lines show the mean of the control responses. Solid horizontal lines show the mean difference between the control and treatment conditions.

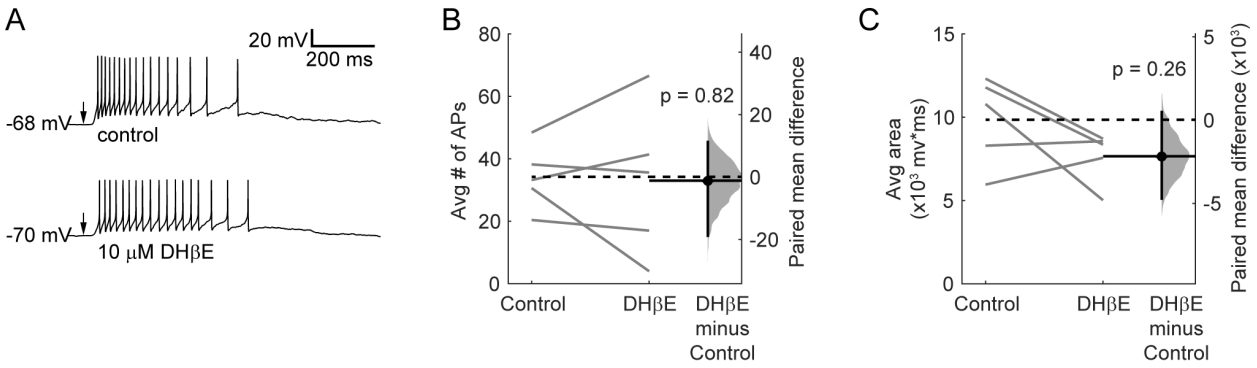

Figure 2-5 $\alpha_4\beta_2$* nAChRs do not mediate the ACh-induced depolarization of VIP neurons.

(A) Example traces show that a spike train elicited by a 10 ms puff of 1 mM ACh (top) was not blocked by 10 μM DHβE (bottom), an $\alpha_4\beta_2$* nAChR antagonist. Arrows indicate the time of the ACh puffs, and voltages indicate resting membrane potential. (B,C) DHβE did not significantly affect the average number of action potentials (B) or the total depolarization (C) elicited by ACh puffs (action potentials: paired independence test, $Z = 0.185$, $p = 0.82$, $n = 5$; area: paired independence test, $Z = 1.40$, $p = 0.26$, $n = 5$). Dashed horizontal lines show the mean of the control responses. Solid horizontal lines show the mean difference between the control and DHβE conditions.

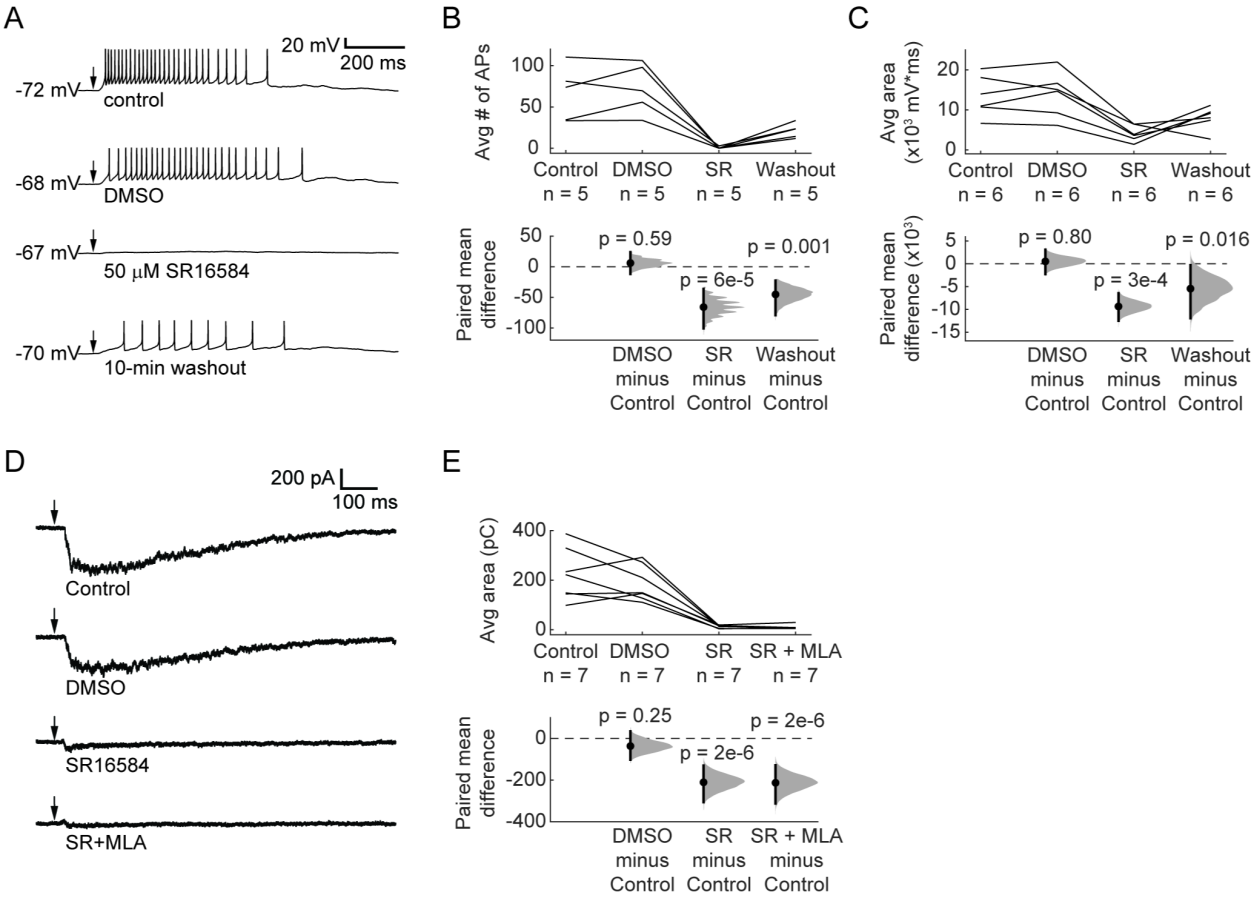

Figure 2-6 ACh-induced depolarization of VIP neurons is predominately mediated by $\alpha_3\beta_4$* nAChRs.

(A) Example traces show that 50 μM SR16584, an $\alpha_3\beta_4$* nAChR antagonist, blocked action potential firing and most of the depolarization elicited by 1 mM ACh puffs. Conditions from top to bottom: control, vehicle (1:1000 DMSO:ACSF), 50 μM SR16584, and 10-min washout (control ACSF). Arrows indicate the time of the ACh puffs, and voltages indicate resting membrane potential. (B) The average number of action potentials elicited by ACh was reduced to 0.64 ± 1.22 (mean ± SD) after bath application of SR16584 (LMM: treatment effect, $F_{3,12} = 20.33$, p = 5e-5, $n = 5$; control vs. DMSO, $t_{12} = 0.55$, $p = 0.59$; control vs. SR, $t_{12} = –6.01$, p = 6e-5; control vs. washout, $t_{12} = –4.13$, $p = 0.001$). (C) The average total depolarization was also significantly decreased by application of SR16584 (LMM: treatment effect, $F_{3,15} = 10.90$, p = 5e-4, $n = 6$; control vs. DMSO, $t_{15} = 0.26$, $p = 0.80$, control vs. SR, $t_{15} = –4.64$, p = 3e-4; control vs. washout, $t_{15} = –2.71$, $p = 0.016$). (D) Example traces show that 50 μM SR16584 blocked nearly all of the inward current elicited by 1 mM ACh puffs. Conditions from top to bottom: control, vehicle (1:1000 DMSO:ACSF), 50 μM SR16584, 50 μM SR16584 + 5 nM MLA. Arrows indicate the time of the ACh puffs. Holding potential was –60 mV. (E) Inward current elicited by ACh was decreased to 7.4 ± 6.2% (mean ± SD) of control by SR16584 (LMM: treatment effect, $F_{3,18} = 27.5$, p = 6e-7, $n = 7$; control vs. DMSO, $t_{18} = –1.20$, $p = 0.25$; control vs. SR, $t_{18} = –6.93$, p = 2e-6; control vs. SR + MLA, $t_{18} = –7.01$, p = 2e-6). (B,C,E) Horizontal dashed lines indicate the level of zero mean difference. Vertical lines on the paired mean difference points indicate 95% bootstrap confidence intervals.

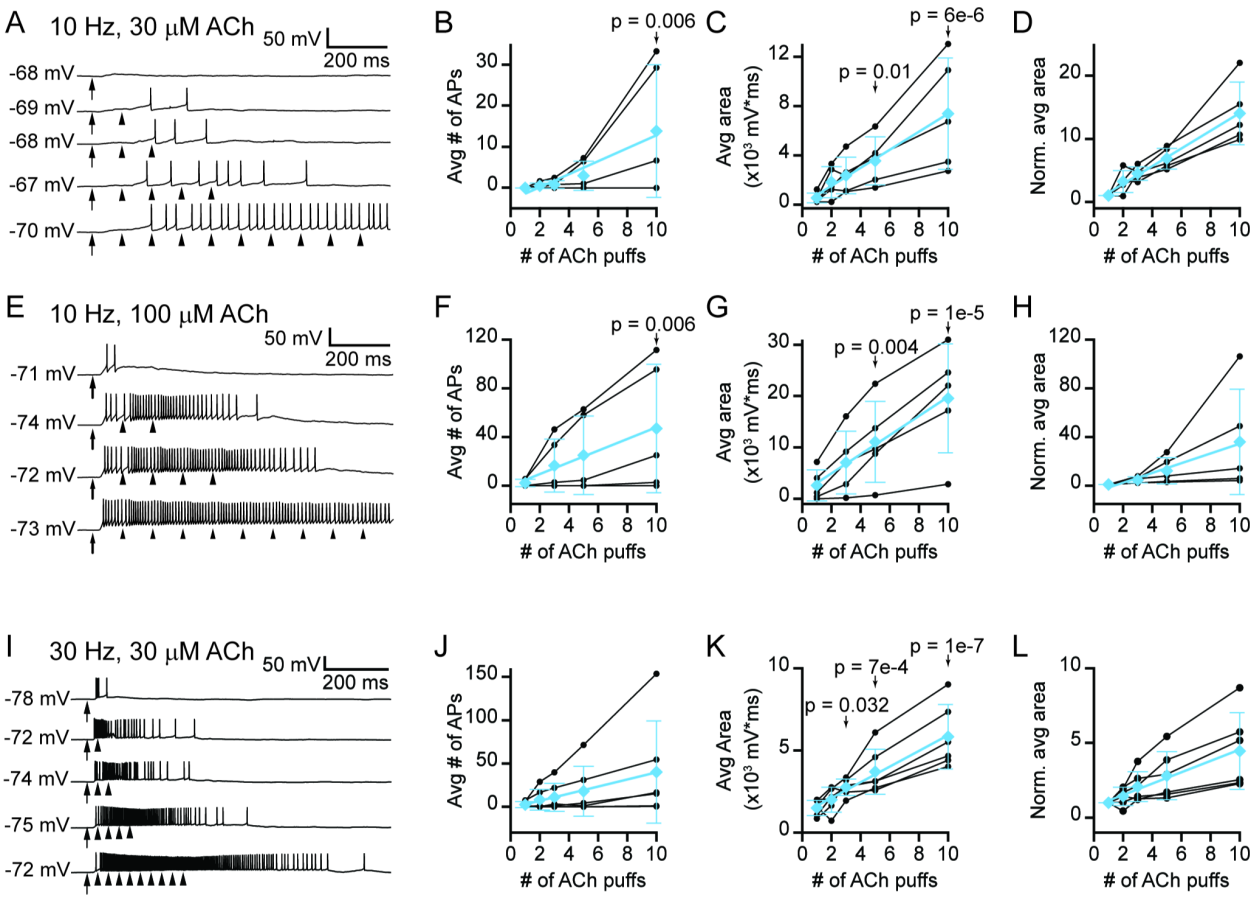

Figure 2-7 Trains of lower concentration ACh puffs elicit temporal summation and spiking in VIP neurons.

Example traces show that 10 Hz trains of 10 ms, 30 μM ACh puffs elicited increased depolarization and probability of firing as the train duration increased from 1 to 10 puffs (top to bottom, respectively). (B) In 3 out of 5 neurons, increasing the number of 30 μM ACh puffs led to spiking. LMM analysis of the responses of all 5 neurons revealed a significant difference in response between 10 puffs and 1 puff (LMM: treatment effect, $F_{4,16} = 3.61$, $p = 0.028$, $n = 5$; 1 puff vs. 2 puffs, $t_{16} = 0.11$, $p = 0.91$; 1 puff vs. 3 puffs, $t_{16} = 0.19$, $p = 0.86$; 1 puff vs. 5 puffs, $t_{16} = 0.68$, $p = 0.51$; 1 puff vs. 10 puffs, $t_{16} = 3.19$, $p = 0.006$). (C,D) In 5 out of 5 neurons, increasing the number of 30 μM ACh puffs progressively increased the absolute (C) or normalized (D) total depolarization, measured as the area under the median-filtered curve, indicating that temporal summation occurred (LMM of absolute values: treatment effect, $F_{4,16} = 12.8$, $p = 7e\text{-}5$, $n = 5$; 1 puff vs. 2 puffs, $t_{16} = 1.23$, $p = 0.24$, 1 puff vs. 3 puffs, $t_{16} = 1.77$, $p = 0.10$; 1 puff vs. 5 puffs, $t_{16} = 2.92$, $p = 0.01$; 1 puff vs. 10 puffs, $t_{16} = 6.63$, $p = 6e\text{-}6$). Cyan data in (B–D) show mean ± SD responses and linear fits to these means [(B), slope = 1.6 APs/puff, $r = 0.97$; (C), slope = 730 mV*ms/puff, $r = 0.99$; (D), slope = 1.4 normalized units/puff, $r = 0.99$]. (E) Example traces show that 10 Hz trains of 10 ms, 100 μM ACh puffs elicited increased depolarization and probability of firing as the train duration increased from 1 to 10 puffs (top to bottom, respectively). (F) In 4 out of 5 neurons, increasing the number of 100 μM ACh puffs led to spiking. LMM analysis of the responses of all 5 neurons revealed a significant difference between 10 puffs and 1 puff (LMM: treatment effect, $F_{3,12} = 3.99$, $p = 0.03$, $n = 5$; 1 puff vs. 3 puffs, $t_{12} = 1.08$, $p = 0.30$; 1 puff vs. 5 puffs, $t_{12} = 1.72$, $p = 0.11$; 1 puff vs. 10 puffs, $t_{12} = 3.38$, $p = 0.006$). (G,H) In 5 out of 5 neurons, increasing the number of 100 μM ACh puffs progressively increased the absolute (G) or normalized (H) total depolarization, measured as the area under the median-filtered curve, indicating that temporal summation occurred (LMM of absolute values: treatment effect, $F_{3,12} = 18.0$, $p = 9.7e\text{-}5$, $n = 5$; 1 puff vs. 3 puffs, $t_{12} = 1.87$, $p = 0.09$; 1 puff vs. 5 puffs, $t_{12} = 3.54$, $p = 0.004$; 1 puff vs. 10 puffs, $t_{12} = 7.07$, $p = 1e\text{-}5$). Cyan data in (F–H) show mean ± SD responses and linear fits to these means [(F), slope = 4.8 APs/puff, $r = 0.99$; (G), slope = 1860 mV*ms/puff, $r = 0.99$; (H), slope = 4.0 normalized units/puff, $r = 0.99$]. (I) Example traces show that 30 Hz trains of 10 ms, 30 μM ACh puffs elicited increased depolarization and probability of firing as the train duration increased from 1 to 10 puffs (top to bottom, respectively). (J) In 4 out of 6

neurons, increasing the number of 30 μM ACh puffs led to increased spiking. However, LMM analysis did not reveal a significant effect of puff number (LMM: treatment effect, $F_{4,20} = 2.70$, $p = 0.06$, $n = 6$). (K,L) In 6 out of 6 neurons, increasing the number of 30 μM ACh puffs progressively increased the absolute (K) or normalized (L) total depolarization, measured as the area under the median-filtered curve, indicating that temporal summation occurred (LMM of absolute values: treatment effect, $F_{4,20} = 19.5$, $p = 1e\text{-}6$, $n = 6$; 1 puff vs. 2 puffs, $t_{20} = 0.92$, $p = 0.37$; 1 puff vs. 3 puffs, $t_{20} = 2.31$, $p = 0.032$; 1 puff vs. 5 puffs, $t_{20} = 4.02$, $p = 7e\text{-}4$; 1 puff vs. 10 puffs, $t_{20} = 7.91$, $p = 1e\text{-}7$). Cyan data in (J–L) show mean ± SD responses and linear fits to these means [(J), slope = 4.1 APs/puff, $r = 0.99$; (K), slope = 480 mV*ms/puff, $r = 0.99$; (L), slope = 0.38 normalized units/puff, $r = 0.99$]. In (A,E,I) arrows and arrowheads indicate the times of ACh puffs, and voltages indicate resting membrane potential. LMM analysis was not run for the normalized data in (D,H,L) since LMM results for the non-normalized data are provided in (C,G,K).

Chapter 3 Vasoactive Intestinal Peptide Modulates the Excitability of Medial Geniculate Neurons in Mice

3.1 Introduction

Neuropeptides are important modulators associated with regulation of processes such as the release of neurotransmitters, vasodilation, inflammation, stress regulation, and metabolism (Gozes & Brenneman, 1989; Kohlmeier & Reiner, 1999; Murphy et al., 1993; Wang et al., 1997). Vasoactive intestinal peptide (VIP), a 28 amino acid peptide is involved in regulatory mechanisms of the central and peripheral nervous systems (Gozes & Brenneman, 1989). The effects of VIP have been examined in the central nervous system (CNS), with studies showing that VIP can modulate intrinsic properties of neurons and even affect synaptic transmission (Gozes & Brenneman, 1989; Kohlmeier & Reiner, 1999; Murphy et al., 1993; Wang et al., 1997). Based on these findings, it is predicted that VIP affects sensory perception. This hypothesis is supported by studies that show expression of VIP receptors (VIPRs) in thalamic relay nuclei (Sheward et al., 1995; Usdin et al., 1994; Vertongen et al., 1997), and evidence showing that VIP strongly excites neurons in somatosensory thalamus (Lee & Cox, 2003; Sun et al., 2003). Activation of VIPRs in thalamic regions is known to shift the voltage-activation curves of hyperpolarization-activated cyclic-nucleotide-gated channels (HCN) toward more depolarized membrane potentials via cyclic adenosine monophosphate (cAMP) signaling cascades, leading to an increase in hyperpolarization-activated cationic currents (I_h) (Lee & Cox, 2003; Sun et al., 2003). Therefore, activation of VIPRs in thalamus is suggested to alter the excitability of neurons via cAMP signaling pathways. The medial geniculate (MG), the auditory

thalamic nucleus, has one of the highest VIPR expression levels in the brain (Hill et al., 1992). Despite the potential that VIP modulates the excitability of thalamic neurons in the MG during auditory processing, the role and source of VIP signaling to the MG remain mostly unknown.

This gap in knowledge has remained due in part to the lack of known sources of VIP signaling to the MG. Previous work by our group identified a population of VIP neurons as the first molecularly identifiable neuron type in the IC (Goyer et al., 2019). Using VIP-IRES-Cre x Ai14 mice, we determined that VIP neurons are glutamatergic and send long range projections to different regions in the auditory pathway including the MG. However, the effects of the synaptic outputs of IC VIP neurons on their downstream targets remain unknown. Based on our previous findings, we are now able to label VIP projections from the IC to the MG in VIP-IRES-Cre x Ai14 mice using retrograde tracing and immunofluorescence techniques. This approach, in combination with current-clamp recordings and pharmacology, positions us to determine the role of VIP signaling in the MG and elucidate the potential sources of VIP signaling to this auditory brain region.

In this study, we hypothesized that VIP signaling modulates the excitability of most MG neurons, and that VIP neurons from the IC provide a major source of VIP signaling to the auditory thalamus. In situ hybridization data showed that most MG neurons express VIP receptor 2 (VIPR2), suggesting that VIP signaling can modulate the excitability of MG neurons via G-protein-coupled receptor (GPCR) mechanisms. Furthermore, we injected Retrobeads, a fluorescent retrograde tracer into the MG and found that the IC and auditory cortex are potential sources of VIP-ergic input to the MG. Using current clamp whole-cell electrophysiology, we found that puff applications of VIP near the cell bodies of most MG neurons led to a long-lasting depolarization. The effect of VIP was unaffected by glutamate and $GABA_A$ receptor antagonists,

while the effect of VIP was significantly decreased by PG 99-465, a VIPR2-specific antagonist. This suggests that VIP modulates the excitability of MG neurons by directly activating VIPRs on the cell, as opposed to modulating the release of a different neurotransmitter from presynaptic terminals. Finally, we found that the neurons affected by VIP during current clamp experiments varied in morphology and location within the MG, suggesting that MG neurons are modulated by VIP signaling regardless of their morphological or intrinsic properties, or their location within the MG subdivisions. Our data reveal that VIP serves as a neuromodulator in the tectothalamic pathway, suggesting an important role for neuropeptide signaling during auditory processing.

3.2 Results

3.2.1 VIPR2 mRNA is heavily expressed in the MG.

The excitability of neurons in somatosensory thalamus is known to be affected by VIP via effects mediated by VIPRs (Lee & Cox, 2003; Sun et al., 2003). Furthermore, early binding studies showed that VIPRs are highly expressed in the MG (Hill et al., 1992). However, the expression and distribution of VIPR mRNA in the MG had not been tested. To address this, we used fluorescent in situ hybridization to determine the expression of *VIPR1* and *VIPR2* mRNA in MG neurons. Based on our previous findings that VIP neurons from the IC send long-range projections to the three major subdivisions of the MG (Beebe et al., 2022; Goyer et al., 2019), we hypothesized that expression of VIPRs would be abundant in all subregions of the MG. We found that *VIPR2* mRNA is strongly expressed in the MG, while no expression of *VIPR1* mRNA was observed in this region (Figure 1). These results suggest that VIPR2 are the main receptors mediating VIP signaling in the MG.

3.2.2 VIP projections to the MG are provided by several brain regions.

The results presented here show that *VIPR2* mRNA is strongly expressed in the MG. However, the potential sources of VIP signaling to the MG remain unknown. We hypothesized that VIP neurons from the IC, auditory cortex, and the reticular thalamic nucleus (RTN), regions that send direct projections to the MG, are sources of VIP signaling to the auditory thalamus. Aside from the VIP projections from the IC uncovered by previous studies (Beebe et al., 2022; Goyer et al., 2019), the auditory cortex is suggested to contain a small population of VIP neurons that send long range projections to the MG (Bertero et al., 2021) and VIP-expressing neurons have been described in the RTN (Burgunder et al., 1999). With the goal of uncovering the sources of VIP to the MG, we performed retrograde tracing by using fluorescent Retrobead injections in the MG of VIP-IRES-Cre x Ai14 mice of both sexes and used confocal imaging to observe retrogradely labeled tdTomato+ neurons in coronal brain slices of the IC, RTN and auditory cortex. Our results showed Retrobeads were present in all 3 regions targeted (Figure 2). In the IC, Retrobeads were found within the central nucleus and dorsal cortex subdivisions. In both subdivisions, we found green Retrobeads co-labeling with tdTomato+, VIP neurons. In the RTN, we found green Retrobeads present, however we did not see any tdTomato+ neurons in RTN, suggesting that VIP neurons are absent in mouse RTN (previous reports of VIP expression in RTN examined rats). Lastly, we found Retrobead-labeled VIP neurons in the auditory cortex, supporting previous evidence for long-range, VIP neuron projections from cortex to the MG. These results suggest that the VIP neurons from the IC and cortex are potential sources of VIP signaling to the MG.

3.2.3 VIP applications drive prolonged depolarization of MG neurons via VIPR activation.

To test the effect of VIP on the excitability of MG neurons, we targeted current clamp recordings to MG neurons in acute thalamocortical brain slices from C57BL/6J mice. Three

second, 500 nM VIP puffs were provided with a puffer pipette approximately 20 μm away and 40 μm above the recorded cell. We found that VIP elicited depolarization in 67 out of 76 MG neurons recorded (88%). The effect of VIP lasted several seconds, suggesting that VIP can increase the excitability of MG neurons for prolonged periods (Figure 3).

Based on previous findings (Hill et al., 1992), and our data showing the strong expression of VIPR2s in the MG, we hypothesized that VIPRs are driving the effect of VIP that we observe on MG neurons. By using pharmacology during our current clamp recordings, we found that the non-selective VIPR antagonist [D-p-Cl-Phe^{6},Leu^{17}]-VIP (500 nM) decreased the effect of VIP on MG neurons (Figure 3), indicating that the elicited depolarization is mediated by VIPRs expressed in the MG.

3.2.4 VIPR2 mediates the effect of VIP on MG neurons.

mRNA expression of VIPRs in the MG suggests that VIPR2 is the only VIPR expressed in the MG. Therefore, we hypothesized that VIPR2 was the main receptor mediating the effect of VIP on MG neurons. We used PG 99-465, a selective VIPR2 antagonist, to elucidate the involvement of VIPR2 in this mechanism. By using current clamp recordings, we found that bath and puff application of 100 nM PG 99-465 led to a decrease in the effect of VIP on the recorded MG neurons (Figure 4). These results suggest that VIPR2 plays an important role in the mechanism for VIP signaling in the MG.

3.2.5 Depolarization of MG neurons by VIP does not require neurotransmitter release from presynaptic inputs.

The MG receives both excitatory and inhibitory inputs (Andersen et al., 1980; Calford & Aitkin, 1983; Jones, 1975; Jones & Rockel, 1971; Kudo & Niimi, 1978; Mellott et al., 2014;

Montero, 1983; Rouiller et al., 1985; Rouiller & de Ribaupierre, 1985). Currently, the effects of VIP signaling on synaptic terminals in the MG remain unexplored. We hypothesized that VIP depolarized presynaptic inputs to MG neurons, leading to glutamate release and the prolonged depolarization observed after VIP applications. To test this, we used pharmacology to block glutamatergic and GABAergic signaling during current clamp recordings. The following drugs were used to block glutamatergic and GABAergic neurotransmission: 10 μM NBQX to block AMPA receptors, 50 μM D-APV to block NMDA receptors, 5 μM gabazine to block $GABA_A$ receptors. After bath application of the synaptic blockers, we observed that the depolarization elicited by 2 μM VIP puffs was not significantly altered, suggesting that the effect of VIP on MG neurons is independent of presynaptic glutamatergic and GABAergic inputs, and instead happening via activation of VIPRs on MG neurons themselves (Figure 5).

3.3 Discussion

In this study, we determined that VIP strongly modulates the excitability of neurons in the auditory thalamus. Our data show that during whole-cell current clamp recordings, VIP applications elicited long-lasting depolarizations in MG neurons. This effect was driven by VIPR2 expressed by MG neurons, as I showed that the mRNA for these receptors is strongly expressed in the MG. This is further supported by the evidence showing that the effect of VIP is not abolished by blockers of ionotropic glutamate and $GABA_A$ receptors (Figure 5). VIP signaling is known to modulate intrinsic properties of thalamocortical neurons in somatosensory cortex (Lee & Cox, 2003; Sun et al., 2003). Our findings support the hypothesis that VIP also affects the intrinsic properties and excitability of neurons in the MG. Furthermore, our retrograde tracing data suggest that VIP neurons in the IC and auditory cortex represent potential sources of VIP signaling to the MG. These results further our knowledge on the potential role of VIP

neurons in the IC and auditory cortex, in which their changes in excitability during auditory processing can lead to changes in their signaling to downstream targets via excitatory or inhibitory neurotransmission, and neuropeptide signaling. Overall, these results uncover a role for VIP signaling as a potent neuromodulator in the auditory pathway.

3.3.1 VIP mediates the excitability of MG neurons via VIPRs.

VIPRs are GPCRs. Studies have documented that VIPR activation in somatosensory thalamus activates hyperpolarization-activated cyclic-nucleotide-gated channels (HCN) via cyclic adenosine monophosphate (cAMP) signaling cascades, leading to an increase in hyperpolarization-activated cationic currents (I_h) (Lee & Cox, 2003; Sun et al., 2003). The presence of VIPRs in the MG suggests that activation of VIPRs during VIP presentations may have a similar downstream effect on I_h, leading to depolarization of the membrane potential of MG neurons. Furthermore, VIP and its receptors modulate the excitability and synaptic transmission of neurons in hippocampus (Wang et al., 1997), axon outgrowth in cortex (Takeuchi et al., 2020), hormonal secretion in the anterior pituitary and hypothalamus (Lam, 1991; Prysor-Jones & Jenkins, 1988), neuron excitability in brainstem (Kohlmeier & Reiner, 1999), and play a role in modulating immune functions in the thymus (Delgado et al., 1999). However, it was unknown whether VIPRs are involved in similar mechanisms in the MG that drive the depolarization observed in this study.

Data from previous studies determined the presence of VIPRs in the MG (Hill et al., 1992; Joo et al., 2004; Sheward et al., 1995). Based on the reported expression levels of these receptors, we hypothesized a major role for VIPRs 1 and 2 in VIP signaling mechanisms. Our data suggests that VIPR2 are predominantly responsible for the long-lasting depolarization elicited by VIP in MG neurons. Interestingly, VIPR2 is a G_s-coupled GPCR. G_s-coupled

receptors are known to activate excitatory pathways via cAMP and PKA activation (Harmar et al., 1998). Furthermore, the in situ hybridization results presented here suggest that in the MG, VIPR2 is expressed at higher levels than VIPR1, supporting our conclusion that VIPR2 plays a major functional role in regulating the excitability of MG neurons.

Our current-clamp electrophysiology data show that most of the effect of VIP on MG neurons is blocked when PG 99-465, a VIPR2-specific antagonist, is present. However, we have not explored the mechanisms responsible for the portion of the response that was resistant to PG 99-465. Interestingly, based on our in situ hybridization data, only VIPR2 seems to be expressed in the MG. It is possible that PACAP receptors are responsible for the remaining depolarization after PG 99-465 application. To address this in future experiments, pharmacology can be used to block PACAP receptors with receptor-specific antagonists during current-clamp recordings to determine their roles in VIP signaling in the MG. This will provide further insight into the mechanisms of VIP signaling and the influence of these receptor subtypes in the excitability of neurons in the auditory thalamus.

Additionally, we identified VIP neurons in the IC and auditory cortex as potential sources of VIP signaling in the MG, opening the door to further studying how VIP neurons can influence auditory processing via neuropeptide signaling to downstream targets. As it has been determined that other neuron types that project to the MG express other neuropeptides, such as NPY neurons in the IC (Silveira et al., 2020), it is important that future studies aim to understand how different neuropeptides can affect the intrinsic physiology and excitability of thalamocortical neurons.

3.3.2 Functional Implications for Auditory Processing

Previous studies have identified roles for VIP signaling in somatosensory thalamus, specifically in long-lasting changes in the resting membrane potential of thalamocortical neurons

(Lee & Cox, 2003; Sun et al., 2003), but the roles of VIP signaling in the MG are less clear. The results in this study raise the possibility that VIP signaling can establish a more depolarized state of neurons in the auditory thalamus, leading to altered processing of auditory information in the MG.

Finally, it remains unknown how the combination of VIP signaling with other neuromodulators can shape the excitability of neurons in the MG. MG neurons receive direct excitatory and inhibitory inputs (Peruzzi et al., 1997). Some inputs release neuromodulators such as acetylcholine, which is known to modulate synaptic inputs to the MG via presynaptic activation of cholinergic receptors (Sottile et al., 2017). Previous data from our lab showed that both excitatory VIP neurons and inhibitory NPY neurons from the IC send long range projections to the different subdivisions of the MG (Goyer et al., 2019; Silveira et al., 2020). The presence of these projections provides a cocktail of neuromodulators to the MG, potentially leading to diverse changes in excitability of thalamic neurons during auditory processing. Our present data on VIP signaling in the MG opens the door to explore how combinations of neuromodulators affect auditory processing, and how these can alter signal processing and behavioral output via changes in intrinsic physiology and excitability of neurons in the auditory pathway.

3.4 Methods

3.4.1 Animals

All experiments were approved by the University of Michigan Institutional Animal Care and Use Committee and were in accordance with NIH guidelines for the care and use of laboratory animals. Mice were kept on a 12-h day/night cycle with ad libitum access to food and water. VIP-IRES-Cre mice (B6J.Cg-Vip$^{tm1(cre)Zjh}$/AreckJ, Jackson Laboratory, stock # 031628)

(NIH Neuroscience Blueprint Cre Driver Network) were crossed with Ai14 reporter mice (B6.Cg-Gt(ROSA)26Sor$^{tm14(CAG–tdTomato)Hze}$/J, Jackson Laboratory, stock #007914) (Madisen et al., 2010) to yield F1 offspring that expressed the fluorescent protein tdTomato in VIP neurons. F1 mice of both sexes, aged P30–P85, were used for experiments. For current-clamp electrophysiology experiments, wildtype C57BL/6J (Jackson Laboratory, stock #000664) of both sexes, aged P30-P80, were used.

3.4.2 Brain Slice Preparation

Whole-cell patch-clamp recordings were performed in acutely prepared brain slices from C57BL/6J mice. Both males (n = 4) and females (n = 9) aged P33-P51 were used in the data presented here. No differences were observed between animals of different sexes. Mice were deeply anesthetized with isoflurane and then rapidly decapitated. The brain was removed, and a tissue block containing the IC was dissected in 34°C ACSF containing the following (in mM): 125 NaCl, 12.5 glucose, 25 $NaHCO_3$, 3 KCl, 1.25 NaH_2PO_4, 1.5 $CaCl_2$ and 1 $MgSO_4$, bubbled to a pH of 7.4 with 5% CO_2 in 95% O_2. 200 μm thalamocortical brain sections (Metherate & Cruikshank, 1999) were cut in 34°C ACSF with a vibrating microtome (VT1200S, Leica Biosystems) and incubated at 34°C for 30 min in ACSF bubbled with 5% CO_2 in 95% O_2. Slices were then incubated at room temperature for at least 30 min before being transferred to the recording chamber. All recordings were targeted at MG neurons, regardless of their location within the MG.

3.4.3 Current-Clamp Electrophysiology

Slices were placed in a recording chamber under a fixed stage upright microscope (BX51WI, Olympus Life Sciences) and were constantly perfused with 34°C ACSF at ~2

ml/min. All recordings were conducted near physiological temperature (34°C). Current-clamp recordings were performed with a BVC-700A patch clamp amplifier (Dagan Corporation). Data were low pass filtered at 10 kHz, sampled at 50 kHz with a National Instruments PCIe-6343 data acquisition board, and acquired using custom written algorithms in Igor Pro. Electrodes were pulled from borosilicate glass (outer diameter 1.5 mm, inner diameter 0.86 mm, Sutter Instrument) to a resistance of 3.5 – 5.0 MΩ using a P-1000 microelectrode puller (Sutter Instrument). The electrode internal solution contained (in mM): 115 K gluconate, 7.73 KCl, 0.5 EGTA, 10 HEPES, 10 Na_2 phosphocreatine, 4 MgATP, 0.3 NaGTP, supplemented with 0.1% biocytin (w/v), pH adjusted to 7.4 with KOH and osmolality to 290 mmol/kg with sucrose. Data were corrected for an 11 mV liquid junction potential.

To test the effect of VIP on the excitability of MG neurons, VIP (human, rat, mouse, rabbit, canine, porcine) (Tocris cat # 1911), was diluted each day from a 2 μM stock in a vehicle solution containing (in mM): 125 NaCl, 3 KCl, 12.5 glucose and 3 HEPES. The solution was balanced to a pH of 7.40 with NaOH. The working concentration of VIP was 500 nM unless stated otherwise. To apply VIP puffs on brain slices, VIP solution was placed in pipettes pulled from borosilicate glass (outer diameter 1.5 mm, inner diameter 0.86 mm, Sutter Instrument) with a resistance of 3.5 – 5.0 MΩ using a P-1000 microelectrode puller (Sutter Instrument) connected to a pressure ejection system built based on the OpenSpritzer design (Forman et al., 2017). The puffer pipette was placed ~ 20-40 μm from the soma of the patched cell, and five 3 s puff applications at 10 psi and 1 min apart were presented per condition. To isolate the receptors mediating the effects of VIP on MG neurons, we bath and puff applied the following drugs individually: 500 nM [D-p-Cl-Phe^{6},Leu^{17}]-VIP (non-selective VIPR antagonist, Tocris cat. #3054), 100 nM PG 99-465 (VIPR2-specific antagonist, Fisher Scientific cat. # 50-194-6730).

All drugs were washed-in for 10 min before testing how the drugs affected the responses of the recorded neurons to VIP puffs. In one experiment, antagonists for $GABA_A$, AMPA, and NMDA receptors were bath applied to isolate direct effects of VIP on MG neurons from possible VIP-induced changes in release from terminals synapsing onto MG neurons. The following drug concentrations were used: 5 μM SR95531 (gabazine, $GABA_A$ receptor antagonist, Hello Bio), 10 μM NBQX disodium salt (AMPA receptor antagonist, Hello Bio), 50 μM D-AP5 (NMDA receptor antagonist, Hello Bio). All drugs were washed-in for 10 min before testing how the drugs affected the responses of the recorded neurons to VIP puffs.

3.4.4 Analysis of Electrophysiological Recordings

Measurements of the area under current clamp depolarizations were made using custom written algorithms in Igor Pro 8 (Wavemetrics). To determine the area under current clamp depolarizations, data were first median filtered using a 4000 sample (80 ms) smoothing window to remove action potentials while leaving the waveform of the underlying slow depolarization intact. The area under the median-filtered depolarization was then calculated using the "Area" function. Responses to the five VIP puffs delivered per neuron per treatment condition were averaged, and these average values were used for the summary analyses.

3.4.5 Fluorescence In Situ Hybridization

Fluorescence in situ hybridization was performed on fresh frozen brain tissue from 3 female C57BL/6J mice (P73) using the RNAScope Multiplex Fluorescent V2 Assay (Advanced Cell Diagnostics, Newark, CA). To prepare fresh frozen brain tissue, mice were first deeply anesthetized with isoflurane. Brains were then rapidly removed by dissection, frozen on dry ice, embedded in a cryo-embedding medium, and frozen at −80 °C. Cryo-embedded brains were

subsequently sectioned using a cryostat at −20 °C to obtain 15 µm-thick coronal sections of the MG. MG sections were placed on microscope slides and stored at −80 °C. The RNAScope assay was run according to the manufacturer's protocol using the Multiplex Fluorescent Reagent Kit v2 (ACD cat. # 323100) and probes targeting mRNA encoding synaptophysin (*Syp*, channel 1 probe, ACD cat. # 426521), vasoactive intestinal peptide receptor 1 (*VIPR1*, channel 2 probe, ACD cat. # 502231-C2), and vasoactive intestinal peptide receptor 2 (*VIPR2*, channel 3 probe, ACD cat. # 465391-C3). In brief, the RNAScope assay began with tissue sections that were fixed in 10% neutral buffered formalin and dehydrated using a series of 50%, 70%, and 100% ethanol. Sections were then treated with hydrogen peroxide for 10 min at room temperature and then with protease IV for 30 min at room temperature. Probes were hybridized, and the hybridize amplification steps were run as follows: AMP 1 for 30 min at 40 °C, AMP 2 for 30 min at 40 °C, and AMP 3 for 15 min at 40 °C. To develop the channel 1 signal, HRP-C1 was applied for 15 min at 40 °C and Opal 520 for 30 min at 40 °C. The same steps were followed for channels 2 and 3, with Opal 570 used for channel 2 and Opal 690 for channel 3. Opal dyes were obtained from Akoya Biosciences (Marlborough, MA). The tissue was counterstained with DAPI for 30 s at room temperature, a coverslip was placed over the sections, and the sections were left to dry overnight. Slides were stored at 4 °C and imaged within 2 weeks after the protocol was finished. Tile-scan images of complete MG sections were collected using a 20× objective and 2.0 µm Z-step size on a Leica TCS SP8 laser scanning confocal microscope. Images of the slices were analyzed using Neurolucida 360 (MBF Bioscience, Williston, VT).

3.4.6 Intracranial Retrobead Injections

To determine the sources of VIP projections to MG neurons we performed retrograde tracing using green, fluorescent Retrobeads (RB, Luma-Fluor, Inc., Naples, FL, USA). Injections

were made into the right MG of 3 VIP-IRES-Cre x Ai14 mice aged P30-P75 of both sexes. Throughout the procedure, mice were anesthetized with isoflurane (1.5%–3%), and their body temperature maintained with a homeothermic heating pad. Mice were injected subcutaneously with the analgesic carprofen (5 mg/kg, CarproJect, Henry Schein Animal Health, Portland, ME, USA). Following this, the scalp was shaved, and a rostro-caudal incision was made to expose the skull. The injection sites were mapped using stereotaxic coordinates relative to the lambda suture, and injection depths were relative to the surface of the skull. The coordinates used were: 3200 µm rostral, 2175 µm lateral, and 2 injections at depths of 3525 and 3375 µm deep. A craniotomy was made above the injection site using a micromotor drill (K 1050, Foredom Electric Co., Bethel, CT, USA) with a 0.5 mm burr (Fine Science Tools, Foster City, CA, USA). 25 nl RB injections were performed at two different depths, for a total of 50 nl.

RBs were injected with a Nanoject III nanoliter injector (Drummond Scientific Company, Broomall, PA, USA) connected to an MP-285 micromanipulator (Sutter Instruments, Novato, CA, USA). Glass injection pipettes were pulled from 1.14 mm outer diameter, 0.53 mm inner diameter capillary glass (cat# 3-000-203-G/X, Drummond Scientific Company) with a P-1000 microelectrode puller (Sutter Instrument). The injector tip was cut, and front-filled with RB. After the injection was complete, the scalp was glued using 3 M Vetbond tissue adhesive (3 M, St. Paul, MN, USA), and the incision was treated with 0.5 ml 2% lidocaine hydrochloride jelly (Akorn Inc., Lake Forest, IL, USA). After recovery from anesthesia, mice were returned to the vivarium and were monitored daily.

Seven days after RB injection, mice were anesthetized with isoflurane and perfused transcardially with phosphate-buffered saline (PBS), pH = 7.4, for 1 min and then with a 10% buffered formalin solution (Millipore Sigma, cat# HT501128, Burlington, MA, USA) for 10 min.

Brains were collected and stored in the same formalin solution for 2 h then saved in PBS overnight at 4°C. Brains were cut into 50 μm coronal sections on a vibratome. Sections were then mounted on Superfrost Plus microscope slides (Thermo Fisher Scientific, catalog #12-550-15, Waltham, MA, USA) and coverslipped using Fluoromount-G (SouthernBiotech, catalog #0100-01, Birmingham, AL, USA).

3.4.7 Retrobead Analysis

Following RB injections, sections were examined for tdTomato+ (VIP) cells and for RB-labeled cells in regions known to contain neurons projecting to the MG (ipsilateral IC, ipsilateral cortex, ipsilateral RTN). Confocal images were taken from a series of coronal sections of the IC, RTN, and cortex and imported into Neurolucida 11 software (MBF Bioscience) for analysis. VIP neurons were identified based on tdTomato fluorescence.

3.4.8 Statistical Analyses

Data analysis and significance tests were performed using custom algorithms combined with statistical functions available in Igor Pro 8 (Wavemetrics), MATLAB R2021a (MathWorks), and R 4.1.0 (The R Project for Statistical Computing). Data were analyzed and are presented following the estimation statistics approach, which emphasizes effect sizes and their confidence intervals over *p* values (Bernard, 2019; Calin-Jageman & Cumming, 2019).

Statistical tests for differences between two groups were made using the "independence_test" function in the "coin" package in R (Hothorn et al., 2006, 2008). The "independence_test" is a non-parametric permutation test based on the theoretical framework of Strasser and Weber (Strasser & Weber, 1999). The "independence_test" was set to use a block design to represent the paired measurements in our data, to perform a two-sided test where the

null hypothesis was zero Pearson correlation, and to generate the conditional null distribution using Monte Carlo resampling with 10,000 iterations.

3.5 Figures

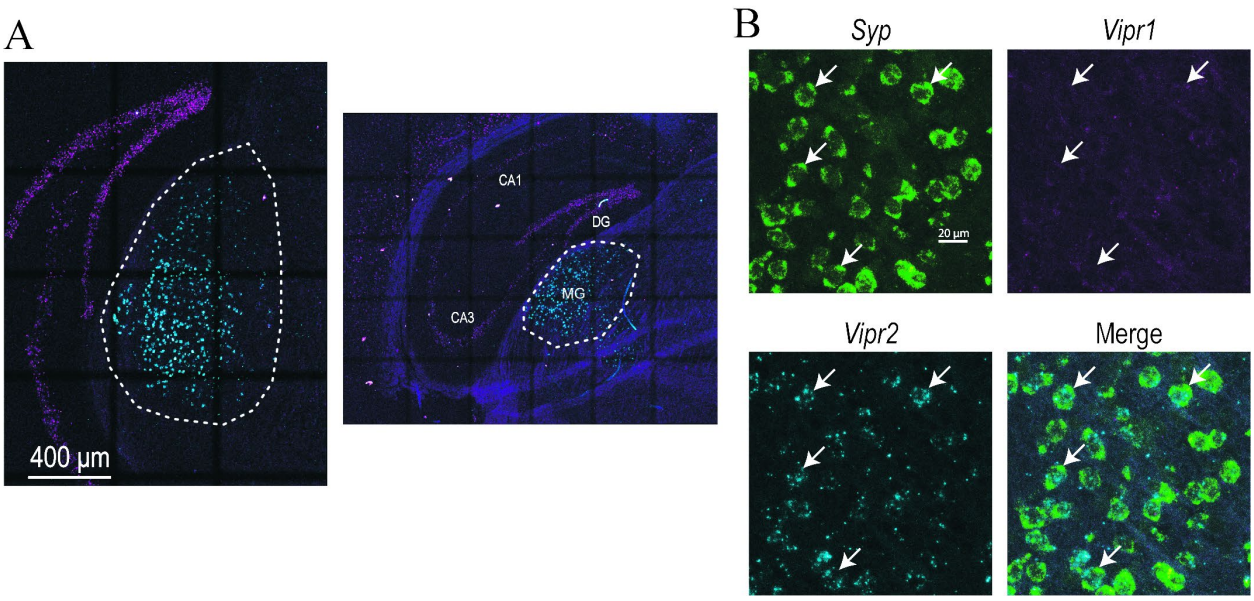

Figure 3-1 VIPR2 mRNA is strongly expressed in the MG.

A) Representative 10x confocal images of the MG (left) and hippocampus (right) showing the distribution of the expression of *VIPR1* (magenta) and *VIPR2* (cyan) mRNA. Dashed lines indicate the borders of the MG. B) Representative 63x images showing the expression of *VIPR1* and *VIPR2* mRNA in *Syp*$^{+}$ MG neurons (green). Arrows point at *Syp*$^{+}$ neurons that also express *VIPR2* mRNA.

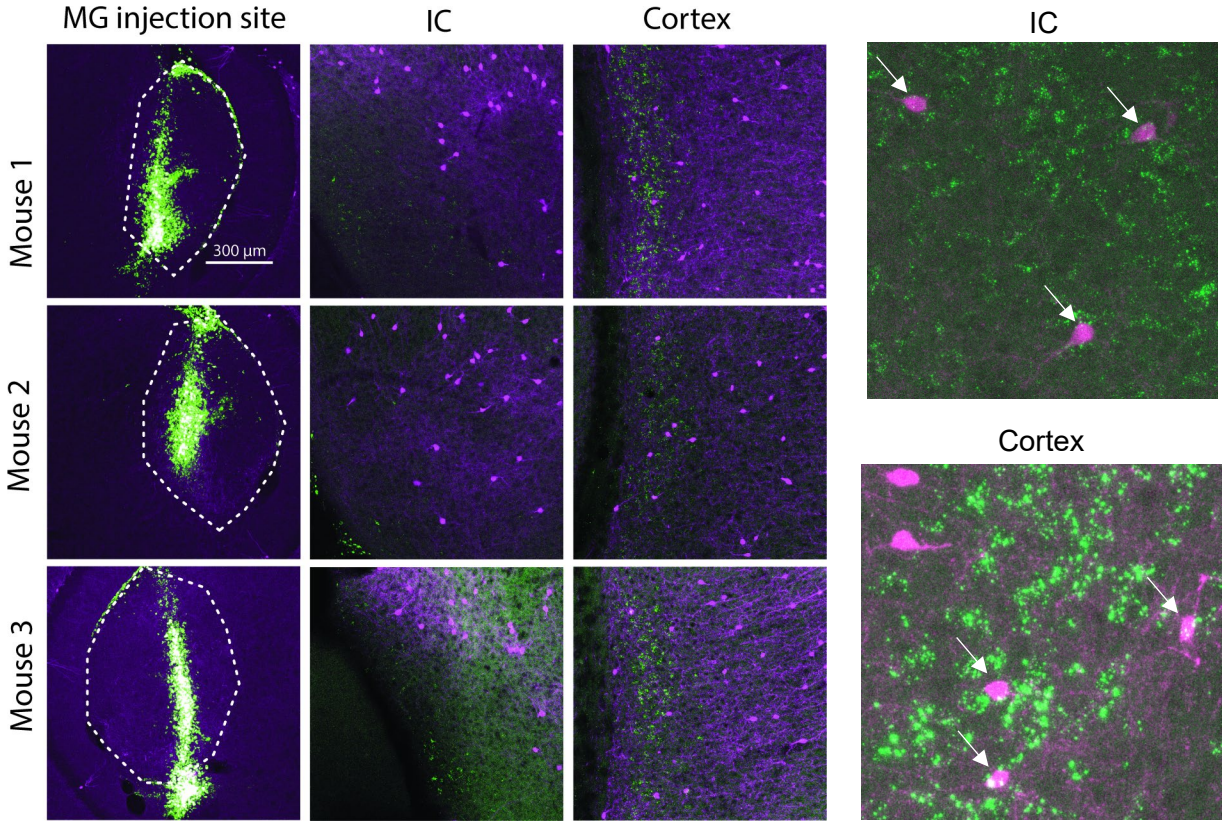

Figure 3-2 The MG receives VIP projections from the IC and auditory cortex.

Representative 10x confocal images of the Retrobead injection sites in the MG, and representative 20x images of Retrobeads present in the IC and cortex of VIP-IRES-Cre x Ai14 mice. The presence of Retrobeads co-labeling with VIP neurons (close-up images on right) in the IC and cortex shows that VIP neurons in these brain regions project to the MG. Arrows indicate tdTomato+ neurons that were positive for Retrobeads.

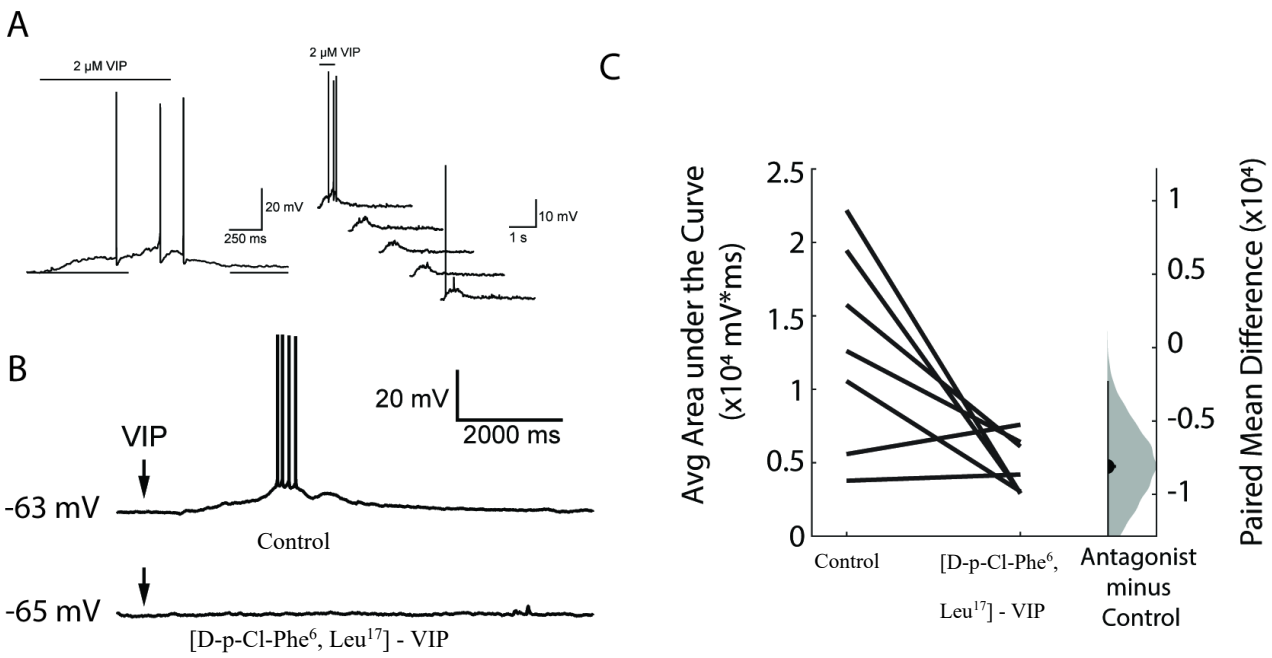

Figure 3-3 VIP applications drive a prolonged depolarization on MG neurons via VIPR activation.

A) Example traces show that VIP puffs (2 µM) elicited a strong, long-lasting depolarization in MG neurons that occasionally led the neuron to fire action potentials. B) Example traces show that the effect of VIP (500 nM) on MG neurons is decreased by the VIPR antagonist [D-p-Cl-Phe^6, Leu^{17}] - VIP (500 nM). C) Treatment with [D-p-Cl-Phe^6, Leu^{17}] - VIP decreased the average area under the median-filtered curve elicited in response to repeated VIP puffs in 5 out of 7 cells (Control: 12800 ± 6800 mV*ms (mean ± SD); Antagonist: 4700 ± 1900 mV*ms, LMM: treatment β = -8100, p = 0.0106, n = 7).

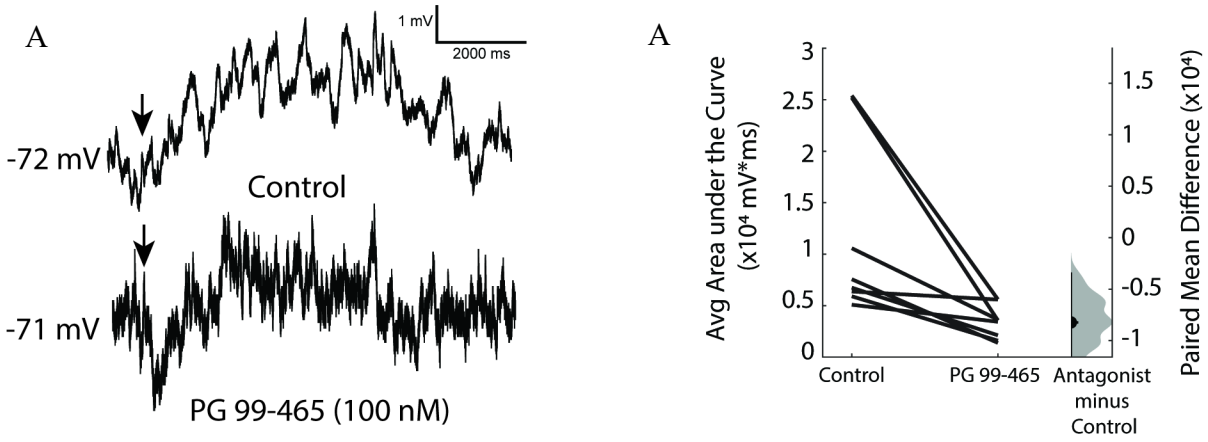

Figure 3-4 VIPR2 mediates the effect of VIP on MG neurons.

A) Example traces show that the effect of VIP (500 nM) on MG neurons is decreased by the VIPR2 antagonist PG 99-465 (100 nM). Arrows indicate time when 3 s VIP puff started. B) Treatment with PG 99-465 decreased the effect of VIP on the average area under the median-filtered curve elicited in response to repeated VIP puffs (Control: 11300 ± 8100 mV*ms; Antagonist: 4700 ± 4300 mV*ms, LMM: treatment β = -8234, p = 0.0223, 97.5% Confidence Intervals (CI) [-14059.786, -2408.248], n = 8).

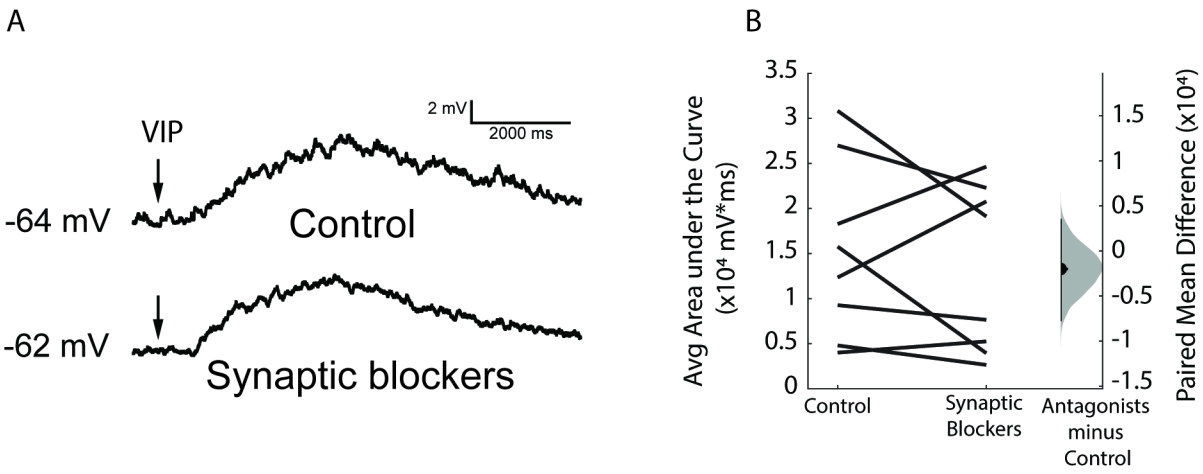

Figure 3-5 The effect of VIP persists after blocking AMPA, NMDA, and $GABA_A$ receptors.

A) Example traces show that VIP puffs (2 μM) elicited depolarization in MG neurons in the presence of NBQX, AP5, and GABAzine. B) Treatment with the synaptic blockers did not abolish the effect of VIP on MG neurons (Control: 15300 ± 9800 mV*ms; Antagonist: 13300 ± 9200 mV*ms, LMM: treatment β = -1999.03, p = 0.4722, 97.5% CI [-7465.131, 3467.063], n = 8).

Chapter 4 Discussion and Future Directions

4.1 Summary of Contribution

In this dissertation, I established several novel effects and mechanisms of acetylcholine and VIP as neuromodulators of the tectothalamic region of the auditory pathway in mice. In Chapter 2, I provided evidence for the first, cellular-level mechanism for cholinergic signaling in the IC. By using brain slice electrophysiology and pharmacology, we uncovered that acetylcholine depolarizes VIP neurons, a principal neuron type in the IC, via $\alpha_3\beta_4$* nAChRs. In Chapter 3, I provided insight on the role and mechanisms of VIP signaling in the excitability of neurons in the auditory thalamus. Our findings uncovered that VIP signaling can regulate the excitability of neurons in the auditory thalamus and provided new insights on the sources of VIP signaling to this region. In this chapter, I will discuss outstanding questions and future experiments that will expand the field's knowledge on neuromodulators and their roles in auditory processing and plasticity mechanisms in the auditory pathway.

4.2 Elucidating the effects and mechanisms of cholinergic modulation in the IC.

Previous studies have determined that cholinergic signaling is important for attention mechanisms, learning, and synaptic plasticity (Irvine, 2010). Even though previous studies have provided evidence for ACh-mediated plasticity in the IC (Ji et al., 2001; Ji & Suga, 2003), the cellular mechanisms for cholinergic signaling in this region remained unknown. My work uncovered a novel mechanism of cholinergic signaling in the IC by determining, for the first time, the cholinergic receptors expressed by a specific type of neuron in this region. In Chapter

2, I showed that ACh causes long-lasting depolarization in VIP neurons in the IC. Since previous studies showed that the PMT sends projections throughout the IC (Motts & Schofield, 2009), it will be important for future studies to determine the effects of ACh on other neuron types in the IC. A potential target for these studies is NPY neurons, an inhibitory neuron type in the IC (Silveira et al., 2020). Understanding the mechanisms of cholinergic signaling in NPY neurons would reveal how ACh differentially affects the excitability of neurons with contrasting neurotransmitter contents. Furthermore, understanding the effects of ACh on VIP and NPY neurons could provide further input on the importance of neuromodulation in the balance of excitatory and inhibitory activity during auditory processing.

A surprising result was finding that $\alpha_3\beta_4$* nAChRs were the main receptors driving the effect of ACh on VIP neurons in the IC. This combination of nicotinic receptor subunits is rather rare in the brain, but it has been shown to be expressed by neurons in the IC (Gahring et al., 2004; Marks et al., 2002, 2006; Salas et al., 2003; Wada et al., 1989; Whiteaker et al., 2002). Furthermore, $\alpha_3\beta_4$* nAChRs have been implicated in nicotine addiction (Beiranvand et al., 2014; Grady et al., 2009; Scholze et al., 2012; Sheffield et al., 2000). In the nicotine-addiction context, α_3-containing nAChRs play a role in nicotine-induced Ca^{2+} increases, leading to changes in cAMP signaling and signal transduction (Di Angelantonio et al., 2011; Pugh et al., 2010; Takahashi et al., 2020). Considering that $\alpha_3\beta_4$* nAChRs have slower kinetics compared to most other nAChRs (David et al., 2010), the results in Chapter 2 suggest that $\alpha_3\beta_4$* nAChRs are capable of exciting neurons for more prolonged periods compared to other nAChRs present in the IC. Further understanding the roles of these receptors in the IC can elucidate the importance of prolonged neuromodulation of neurons in the auditory system and its effects on auditory processing.

Repeated presentations of ACh were found to promote temporal summation and firing in VIP neurons, even at lower ACh concentrations. We recently showed that VIP neurons are contacted by numerous cholinergic boutons along their dendrites and cell bodies, suggesting that VIP neurons in the IC may be strongly impacted by cholinergic signaling (Kwapiszewski et al., 2023). Thus, our results showing temporal summation in these neurons suggest that this may be a mechanism that is commonplace in the IC, which receives prominent cholinergic inputs. However, we have not explored this phenomenon in vivo. It is known that cholinergic PMT neurons in vivo typically have low firing rates, but behavioral states such as arousal can rapidly increase the rate of firing (Reese et al., 1995a, 1995b; Sakai, 2012). Future studies can explore how trains of cholinergic input to the IC affect neuronal excitability by using optogenetics to stimulate PMT cholinergic terminals in the IC in an awake animal while recording neuron activity in the IC. Currently, mice that express the Channelrhodopsin (ChR2) protein on cholinergic neurons are possible by crossing the commercially available ChAT-Cre mouse (Rossi et al., 2011) with the Ai32 mouse (Madisen et al., 2010). ChR2 is a light-sensitive ion channel that when activated can induce neurotransmitter release from the neurons expressing it. With this approach, it is possible to test how ACh release from PMT terminals in the IC impacts the excitability of VIP neurons and other IC neurons in vivo. This will elucidate the importance of repeated cholinergic input to the IC, while also providing information on the importance of the rate of cholinergic signaling in the auditory system in diverse behavioral states.

Finally, the effects of acetylcholine on specific neuron populations in the IC in vivo remain unexplored. The results presented here are based on exogenous applications of ACh onto VIP neurons in slice preparations. To further understand the mechanisms of ACh in the auditory pathway, examining endogenous release of ACh will be an important next step. For the purposes

of this study, a mouse model expressing ChR2 on cholinergic neurons of the PMT will help elucidate the effects of endogenous ACh release onto neurons in the IC. Furthermore, by performing auditory learning tasks during activation of cholinergic neurons, the effects of ACh on auditory processing and plasticity in the IC can be further understood. The results presented in Chapter 2 provide the fundamental knowledge to further understand the role of ACh as a neuromodulator in the IC and within the central auditory pathway.

4.3 Uncovering the roles and sources of VIP signaling in the auditory thalamus.

Neuropeptide signaling is suggested to modulate the excitability of neuronal populations during sensory processing. In somatosensory thalamus, VIP signaling enhances the excitability of neurons via activation of local VIPRs (Lee & Cox, 2003; Sun et al., 2003). However, the effects of VIP in the MG were unknown. In Chapter 3, I uncovered that VIP elicits a depolarizing response in MG neurons, similar to what has been observed in somatosensory thalamus. This shows that VIP signaling in the MG could be playing an important, and previously unappreciated, role in modulating the responses of MG neurons to incoming stimuli. Currently, the data obtained is based on exogenous applications of VIP to the MG, and it is yet to be observed whether endogenous release of VIP promotes a similar effect on MG neurons. To address this, further knowledge is required on the mechanisms of VIP signaling in the MG, as well as the sources of VIP inputs to this region, which were unknown. Here, I discuss my findings on the receptors and the potential sources of VIP signaling to the MG, opening the door to future studies on endogenous VIP signaling and its modulatory roles during in vivo processing of auditory cues.

Studies have determined that neurons in the MG strongly express VIPRs (Hill et al., 1992; Joo et al., 2004; Sheward et al., 1995). By using pharmacology during current-clamp

recordings, I uncovered that VIPR2 mediates most of the depolarizing effect of VIP on MG neurons. Interestingly, activation of VIPRs in thalamic regions is known to activate hyperpolarization-activated cyclic-nucleotide-gated channels (HCN) via cyclic adenosine monophosphate (cAMP) signaling cascades, leading to an increase in hyperpolarization-activated cationic currents (I_h) (Lee & Cox, 2003; Sun et al., 2003). The results presented in Chapter 3 suggest that activation of VIPR2 during VIP presentations may have a similar downstream effect on I_h and therefore depolarizing the membrane potential of MG neurons. Finally, in some cases during current-clamp recordings, MG neurons treated with VIPR antagonists hyperpolarized during the treatment. A potential explanation for this phenomenon is that there is tonic release of VIP onto MG neurons, suggesting a constant modulatory effect of VIP in this region. Additional experiments are required to test whether this is the case. Overall, my results provide new insight on the potential role of VIP as a neuromodulator capable of changing the excitability of MG neurons and thereby altering sensory processing and relay of auditory information to the cortex. These results also provide a stepping stone to studying this in vivo, where the effects of VIP in the MG remain unknown.

The sources of VIP signaling to the MG were unknown. Here, we uncovered two potential sources of VIP signaling to the MG: VIP neurons in the IC and VIP neurons in the auditory cortex. These results support previous findings showing that VIP neurons from the IC and auditory cortex send long-range projections to other subcortical targets, such as the MG (Bertero et al., 2021; Goyer et al., 2019). Furthermore, these results suggest that the MG receives VIP signaling from inhibitory and excitatory VIP neuron classes. The combination of these inputs, along with other neuromodulatory mechanisms known to happen in the MG, could result in the alteration of the excitability of neurons responsible for processing auditory information

before it is relayed to cortex. Lastly, the distribution of VIP inputs from IC and cortex in the MG has been observed by several groups but requires further exploration (Beebe et al., 2022; Bertero et al., 2021; Goyer et al., 2019). Future studies are needed to determine if there is a difference between the distribution of VIP inputs from IC and cortex within the MG, and how the interaction between them leads to changes in the excitability of MG neurons. With previous studies showing that there are neurons with varying intrinsic characteristics in the MG (Bartlett & Smith, 1999), the results presented here could be pointing at differences of VIP input depending on intrinsic properties and location of postsynaptic neurons within the MG.

4.4 Implications for understanding neuromodulation in the auditory pathway.

Current hearing loss treatments have varying degrees of success in patients, with some patients not benefiting from the available options (Blamey et al., 1996; Boisvert et al., 2020). Studies through the years have determined that during hearing loss, the IC and other auditory brain regions can undergo synaptic plasticity, suggesting that the circuit itself is compensating for the loss of sensory input (Chambers et al., 2016; Kim et al., 2004; Moore & Kowalchuk, 1988; Mossop et al., 2000; Robertson & Irvine, 1989). Even though it has been suggested that neuromodulators such as ACh can promote synaptic plasticity in several brain regions, the mechanisms involved in plasticity remain largely unknown in the tectothalamic pathway. The results described in the present study provide evidence for the different mechanisms that neuromodulators can use to promote changes in the excitability of neuron populations during the processing of auditory cues. Furthermore, these results open the door to studying the effects of neuromodulators in different neuron types, which can lead to further understanding how modulation of different neuronal populations leads to local excitability changes that can later affect the excitability of postsynaptic targets. Therefore, these findings can further our

understanding of how auditory learning and synaptic plasticity happen in normal hearing animals, as well as provide initial data on how these mechanisms can happen under hearing loss conditions. This, along with future studies, can spark the generation of new approaches for hearing loss treatments, and potentially help develop better treatments that can benefit more patients with hearing impairments.

4.5 Concluding remarks

In this body of work, I described cellular-level mechanisms underlying cholinergic signaling in the IC and VIP signaling in the MG. At subcortical levels of the auditory pathway, these neuromodulators appear to be playing an important role in regulating the excitability of neurons. However, the roles of these signaling molecules in auditory processing are yet to be explored in vivo. This study furthers our fundamental understanding of the auditory system, and along with the proposed future studies, it opens the possibility for novel approaches to treat hearing loss and other communication disorders via the manipulation of neuromodulatory signals within the auditory circuitry.

Bibliography

Adams, J. C. (1979). Ascending projections to the inferior colliculus. *Journal of Comparative Neurology*, *183*(3), 519–538. https://doi.org/10.1002/cne.901830305

Aitkin, L. (1991). Rate-level functions of neurons in the inferior colliculus of cats measured with the use of free-field sound stimuli. *Journal of Neurophysiology*, *65*(2), 383–392. https://doi.org/10.1152/jn.1991.65.2.383

Aitkin, L. M., & Martin, R. L. (1987). The representation of stimulus azimuth by high best-frequency azimuth-selective neurons in the central nucleus of the inferior colliculus of the cat. *Journal of Neurophysiology*, *57*(4), 1185–1200. https://doi.org/10.1152/jn.1987.57.4.1185

Aitkin, L., Tran, L., & Syka, J. (1994). The responses of neurons in subdivisions of the inferior colliculus of cats to tonal, noise and vocal stimuli. *Experimental Brain Research*, *98*(1), 53–64. https://doi.org/10.1007/BF00229109

Anand, R., Nelson, M. E., Gerzanich, V., Wells, G. B., & Lindstrom, J. (1998). Determinants of Channel Gating Located in the N-Terminal Extracellular Domain of Nicotinic α7 Receptor. *Journal of Pharmacology and Experimental Therapeutics*, *287*(2), 469–479.

Andersen, R. A., Roth, G. L., Aitkin, L. M., & Merzenich, M. M. (1980). The efferent projections of the central nucleus and the pericentral nucleus of the inferior colliculus in the cat. *The Journal of Comparative Neurology*, *194*(3), 649–662. https://doi.org/10.1002/cne.901940311

Arroyo, S., Bennett, C., Aziz, D., Brown, S. P., & Hestrin, S. (2012). Prolonged Disynaptic Inhibition in the Cortex Mediated by Slow, Non-α7 Nicotinic Excitation of a Specific Subset of Cortical Interneurons. *Journal of Neuroscience*, *32*(11), 3859–3864. https://doi.org/10.1523/JNEUROSCI.0115-12.2012

Askew, C. E., Lopez, A. J., Wood, M. A., & Metherate, R. (2019). Nicotine excites VIP interneurons to disinhibit pyramidal neurons in auditory cortex. *Synapse*, e22116. https://doi.org/10.1002/syn.22116

Askew, C., Intskirveli, I., & Metherate, R. (2017). Systemic Nicotine Increases Gain and Narrows Receptive Fields in A1 via Integrated Cortical and Subcortical Actions. *ENeuro*, *4*(3). https://doi.org/10.1523/ENEURO.0192-17.2017

Ayala, Y. A., & Malmierca, M. S. (2015). Cholinergic Modulation of Stimulus-Specific Adaptation in the Inferior Colliculus. *The Journal of Neuroscience: The Official Journal of the Society for Neuroscience*, *35*(35), 12261–12272. https://doi.org/10.1523/JNEUROSCI.0909-15.2015

Bartlett, E. L., & Smith, P. H. (1999). Anatomic, Intrinsic, and Synaptic Properties of Dorsal and Ventral Division Neurons in Rat Medial Geniculate Body. *Journal of Neurophysiology*, *81*(5), 1999–2016. https://doi.org/10.1152/jn.1999.81.5.1999

Bates, D., Mächler, M., Bolker, B., & Walker, S. (2015). Fitting Linear Mixed-Effects Models Using lme4. *Journal of Statistical Software*, *67*(1), 1–48. https://doi.org/10.18637/jss.v067.i01

Beebe, N. L., & Schofield, B. R. (2021). Cholinergic boutons are closely associated with excitatory cells and four subtypes of inhibitory cells in the inferior colliculus. *Journal of Chemical Neuroanatomy*, *116*, 101998. https://doi.org/10.1016/j.jchemneu.2021.101998

Beebe, N. L., Silveira, M. A., Goyer, D., Noftz, W. A., Roberts, M. T., & Schofield, B. R. (2022). Neurotransmitter phenotype and axonal projection patterns of VIP-expressing neurons in the inferior colliculus. *Journal of Chemical Neuroanatomy*, *126*, 102189. https://doi.org/10.1016/j.jchemneu.2022.102189

Beiranvand, F., Zlabinger, C., Orr-Urtreger, A., Ristl, R., Huck, S., & Scholze, P. (2014). Nicotinic acetylcholine receptors control acetylcholine and noradrenaline release in the rodent habenulo-interpeduncular complex. *British Journal of Pharmacology*, *171*(23), 5209–5224. https://doi.org/10.1111/bph.12841

Bennett, C., Arroyo, S., Berns, D., & Hestrin, S. (2012). Mechanisms Generating Dual-Component Nicotinic EPSCs in Cortical Interneurons. *The Journal of Neuroscience*, *32*(48), 17287–17296. https://doi.org/10.1523/JNEUROSCI.3565-12.2012

Bernard, C. (2019). Changing the Way We Report, Interpret, and Discuss Our Results to Rebuild Trust in Our Research. *ENeuro*, *6*(4). https://doi.org/10.1523/ENEURO.0259-19.2019

Bertero, A., Garcia, C., & Apicella, A. junior. (2021). Corticofugal VIP Gabaergic Projection Neurons in the Mouse Auditory and Motor Cortex. *Frontiers in Neural Circuits*, *15*, 714780. https://doi.org/10.3389/fncir.2021.714780

Bieszczad, K. M., Kant, R., Constantinescu, C. C., Pandey, S. K., Kawai, H. D., Metherate, R., Weinberger, N. M., & Mukherjee, J. (2012). Nicotinic acetylcholine receptors in rat forebrain that bind 18F-nifene: Relating PET imaging, autoradiography and behavior. *Synapse (New York, N.y.)*, *66*(5), 418–434. https://doi.org/10.1002/syn.21530

Blamey, P., Arndt, P., Bergeron, F., Bredberg, G., Brimacombe, J., Facer, G., Larky, J., Lindström, B., Nedzelski, J., Peterson, A., Shipp, D., Staller, S., & Whitford, L. (1996).

Factors affecting auditory performance of postlinguistically deaf adults using cochlear implants. *Audiology & Neuro-Otology*, *1*(5), 293–306. https://doi.org/10.1159/000259212

Boisvert, I., Reis, M., Au, A., Cowan, R., & Dowell, R. C. (2020). Cochlear implantation outcomes in adults: A scoping review. *PLoS ONE*, *15*(5), e0232421. https://doi.org/10.1371/journal.pone.0232421

Boucetta, S., Cissé, Y., Mainville, L., Morales, M., & Jones, B. E. (2014). Discharge Profiles across the Sleep–Waking Cycle of Identified Cholinergic, GABAergic, and Glutamatergic Neurons in the Pontomesencephalic Tegmentum of the Rat. *The Journal of Neuroscience*, *34*(13), 4708–4727. https://doi.org/10.1523/JNEUROSCI.2617-13.2014

Brunso-Bechtold, J. K., Thompson, G. C., & Masterton, R. B. (1981). HRP study of the organization of auditory afferents ascending to central nucleus of inferior colliculus in cat. *Journal of Comparative Neurology*, *197*(4), 705–722. https://doi.org/10.1002/cne.901970410

Calford, M. B., & Aitkin, L. M. (1983). Ascending projections to the medial geniculate body of the cat: Evidence for multiple, parallel auditory pathways through thalamus. *The Journal of Neuroscience: The Official Journal of the Society for Neuroscience*, *3*(11), 2365–2380. https://doi.org/10.1523/JNEUROSCI.03-11-02365.1983

Calin-Jageman, R. J., & Cumming, G. (2019). Estimation for Better Inference in Neuroscience. *ENeuro*, *6*(4). https://doi.org/10.1523/ENEURO.0205-19.2019

Castro, N. G., & Albuquerque, E. X. (1993). Brief-lifetime, fast-inactivating ion channels account for the α-bungarotoxin-sensitive nicotinic response in hippocampal neurons. *Neuroscience Letters*, *164*(1), 137–140. https://doi.org/10.1016/0304-3940(93)90876-M

Chambers, A. R., Resnik, J., Yuan, Y., Whitton, J. P., Edge, A. S., Liberman, M. C., & Polley, D. B. (2016). Central Gain Restores Auditory Processing following Near-Complete Cochlear Denervation. *Neuron*, *89*(4), 867–879. https://doi.org/10.1016/j.neuron.2015.12.041

Christophe, E., Roebuck, A., Staiger, J. F., Lavery, D. J., Charpak, S., & Audinat, E. (2002). Two types of nicotinic receptors mediate an excitation of neocortical layer I interneurons. *Journal of Neurophysiology*, *88*(3), 1318–1327. https://doi.org/10.1152/jn.2002.88.3.1318

Clarke, P., Schwartz, R., Paul, S., Pert, C., & Pert, A. (1985). Nicotinic binding in rat brain: Autoradiographic comparison of [3H]acetylcholine, [3H]nicotine, and [125I]-alpha-bungarotoxin. *The Journal of Neuroscience*, *5*(5), 1307–1315. https://doi.org/10.1523/JNEUROSCI.05-05-01307.1985

d'Incamps, B. L., Krejci, E., & Ascher, P. (2012). Mechanisms Shaping the Slow Nicotinic Synaptic Current at the Motoneuron–Renshaw Cell Synapse. *The Journal of Neuroscience*, *32*(24), 8413–8423. https://doi.org/10.1523/JNEUROSCI.0181-12.2012

Dani, J. A., & Bertrand, D. (2007). Nicotinic acetylcholine receptors and nicotinic cholinergic mechanisms of the central nervous system. *Annual Review of Pharmacology and Toxicology*, *47*, 699–729. https://doi.org/10.1146/annurev.pharmtox.47.120505.105214

David, R., Ciuraszkiewicz, A., Simeone, X., Orr-Urtreger, A., Papke, R. L., McIntosh, J. M., Huck, S., & Scholze, P. (2010). Biochemical and functional properties of distinct nicotinic acetylcholine receptors in the superior cervical ganglion of mice with targeted deletions of nAChR subunit genes. *The European Journal of Neuroscience*, *31*(6), 978–993. https://doi.org/10.1111/j.1460-9568.2010.07133.x

Davison, A. C., & Hinkley, D. V. (1997). *Bootstrap Methods and their Application*. Cambridge University Press. https://doi.org/10.1017/CBO9780511802843

Delgado, M., Martinez, C., Leceta, J., & Gomariz, R. P. (1999). Vasoactive intestinal peptide in thymus: Synthesis, receptors and biological actions. *Neuroimmunomodulation*, *6*(1–2), 97–107. https://doi.org/10.1159/000026369

Di Angelantonio, S., Piccioni, A., Moriconi, C., Trettel, F., Cristalli, G., Grassi, F., & Limatola, C. (2011). Adenosine A2A receptor induces protein kinase A-dependent functional modulation of human α3β4 nicotinic receptor. *The Journal of Physiology*, *589*(Pt 11), 2755–2766. https://doi.org/10.1113/jphysiol.2011.207282

Disney, A. A., Aoki, C., & Hawken, M. J. (2007). Gain modulation by nicotine in macaque v1. *Neuron*, *56*(4), 701–713. https://doi.org/10.1016/j.neuron.2007.09.034

Dodge, F. A., & Rahamimoff, R. (1967). Co-operative action of calcium ions in transmitter release at the neuromuscular junction. *The Journal of Physiology*, *193*(2), 419–432.

Ehret, G., & Merzenich, M. M. (1988). Complex sound analysis (frequency resolution, filtering and spectral integration) by single units of the inferior colliculus of the cat. *Brain Research*, *472*(2), 139–163. https://doi.org/10.1016/0165-0173(88)90018-5

Farley, G. R., Morley, B. J., Javel, E., & Gorga, M. P. (1983). Single-unit responses to cholinergic agents in the rat inferior colliculus. *Hearing Research*, *11*(1), 73–91. https://doi.org/10.1016/0378-5955(83)90046-1

Felix, R. A., Chavez, V. A., Novicio, D. M., Morley, B. J., & Portfors, C. V. (2019). Nicotinic acetylcholine receptor subunit α 7 -knockout mice exhibit degraded auditory temporal processing. *Journal of Neurophysiology*, *122*(2), 451–465. https://doi.org/10.1152/jn.00170.2019

Fitzpatrick, D., Diamond, I. T., & Raczkowski, D. (1989). Cholinergic and monoaminergic innervation of the cat's thalamus: Comparison of the lateral geniculate nucleus with other principal sensory nuclei. *The Journal of Comparative Neurology*, *288*(4), 647–675. https://doi.org/10.1002/cne.902880411

Forman, C. J., Tomes, H., Mbobo, B., Burman, R. J., Jacobs, M., Baden, T., & Raimondo, J. V. (2017). Openspritzer: An open hardware pressure ejection system for reliably delivering picolitre volumes. *Scientific Reports*, *7*(1), Article 1. https://doi.org/10.1038/s41598-017-02301-2

Frisina, R. D., Walton, J. P., Lynch-Armour, M. A., & Byrd, J. D. (1998). Inputs to a physiologically characterized region of the inferior colliculus of the young adult CBA mouse. *Hearing Research*, *115*(1), 61–81. https://doi.org/10.1016/S0378-5955(97)00176-7

Gahring, L. C., Persiyanov, K., & Rogers, S. W. (2004). Neuronal and astrocyte expression of nicotinic receptor subunit β4 in the adult mouse brain. *Journal of Comparative Neurology*, *468*(3), 322–333. https://doi.org/10.1002/cne.10942

Gerzanich, V., Wang, F., Kuryatov, A., & Lindstrom, J. (1998). Alpha 5 Subunit alters desensitization, pharmacology, Ca++ permeability and Ca++ modulation of human neuronal alpha 3 nicotinic receptors. *The Journal of Pharmacology and Experimental Therapeutics*, *286*(1), 311–320.

Gillet, C., Goyer, D., Kurth, S., Griebel, H., & Kuenzel, T. (2018). Cholinergic innervation of principal neurons in the cochlear nucleus of the Mongolian gerbil. *The Journal of Comparative Neurology*, *526*(10), 1647–1661. https://doi.org/10.1002/cne.24433

Goyer, D., Kurth, S., Gillet, C., Keine, C., Rübsamen, R., & Kuenzel, T. (2016). Slow Cholinergic Modulation of Spike Probability in Ultra-Fast Time-Coding Sensory Neurons. *ENeuro*, *3*(5). https://doi.org/10.1523/ENEURO.0186-16.2016

Goyer, D., Silveira, M. A., George, A. P., Beebe, N. L., Edelbrock, R. M., Malinski, P. T., Schofield, B. R., & Roberts, M. T. (2019). A novel class of inferior colliculus principal neurons labeled in vasoactive intestinal peptide-Cre mice. *ELife*, *8*, e43770. https://doi.org/10.7554/eLife.43770

Gozes, I., & Brenneman, D. E. (1989). VIP: Molecular biology and neurobiological function. *Molecular Neurobiology*, *3*(4), 201–236. https://doi.org/10.1007/BF02740606

Grady, S. R., Moretti, M., Zoli, M., Marks, M. J., Zanardi, A., Pucci, L., Clementi, F., & Gotti, C. (2009). Rodent Habenulo–Interpeduncular Pathway Expresses a Large Variety of Uncommon nAChR Subtypes, But Only the α3β4 and α3β3β4 Subtypes Mediate Acetylcholine Release. *The Journal of Neuroscience*, *29*(7), 2272–2282. https://doi.org/10.1523/JNEUROSCI.5121-08.2009

Groot-Kormelink, P. J., Boorman, J. P., & Sivilotti, L. G. (2001). Formation of functional α3β4α5 human neuronal nicotinic receptors in Xenopus oocytes: A reporter mutation approach. *British Journal of Pharmacology*, *134*(4), 789–796. https://doi.org/10.1038/sj.bjp.0704313

Habbicht, H., & Vater, M. (1996). A microiontophoretic study of acetylcholine effects in the inferior colliculus of horseshoe bats: Implications for a modulatory role. *Brain Research*, *724*(2), 169–179. https://doi.org/10.1016/0006-8993(96)00224-7

Happe, H. K., & Morley, B. J. (2004). Distribution and postnatal development of α7 nicotinic acetylcholine receptors in the rodent lower auditory brainstem. *Developmental Brain Research*, *153*(1), 29–37. https://doi.org/10.1016/j.devbrainres.2004.07.004

Harkrider, A. W., & Hedrick, M. S. (2005). Acute effect of nicotine on auditory gating in smokers and non-smokers. *Hearing Research*, *202*(1), 114–128. https://doi.org/10.1016/j.heares.2004.11.009

HARMAR, A. J., ARIMURA, A., GOZES, I., JOURNOT, L., LABURTHE, M., PISEGNA, J. R., RAWLINGS, S. R., ROBBERECHT, P., SAID, S. I., SREEDHARAN, S. P., WANK, S. A., & WASCHEK, J. A. (1998). International Union of Pharmacology. XVIII. Nomenclature of Receptors for Vasoactive Intestinal Peptide and Pituitary Adenylate Cyclase-Activating Polypeptide. *Pharmacological Reviews*, *50*(2), 265–270.

Heckman, C. J., Mottram, C., Quinlan, K., Theiss, R., & Schuster, J. (2009). Motoneuron excitability: The importance of neuromodulatory inputs. *Clinical Neurophysiology : Official Journal of the International Federation of Clinical Neurophysiology*, *120*(12), 2040–2054. https://doi.org/10.1016/j.clinph.2009.08.009

Higley, M. J., & Sabatini, B. L. (2010). Competitive regulation of synaptic Ca influx by D2 dopamine and A2A adenosine receptors. *Nature Neuroscience*, *13*(8), 958–966. https://doi.org/10.1038/nn.2592

Hill, J. M., Harris, A., & Hilton-Clarke, D. I. (1992). Regional distribution of guanine nucleotide-sensitive and guanine nucleotide-insensitive vasoactive intestinal peptide receptors in rat brain. *Neuroscience*, *48*(4), 925–932. https://doi.org/10.1016/0306-4522(92)90280-F

Ho, J., Tumkaya, T., Aryal, S., Choi, H., & Claridge-Chang, A. (2019). Moving beyond P values: Data analysis with estimation graphics. *Nature Methods*, *16*(7), 565–566. http://dx.doi.org.proxy.lib.umich.edu/10.1038/s41592-019-0470-3

Hothorn, T., Hornik, K., Wiel, M. A. van de, & Zeileis, A. (2006). A Lego System for Conditional Inference. *The American Statistician*, *60*(3), 257–263. https://doi.org/10.1198/000313006X118430

Hothorn, T., Hornik, K., Wiel, M. A. van de, & Zeileis, A. (2008). Implementing a Class of Permutation Tests: The coin Package. *Journal of Statistical Software*, *28*(1), Article 1. https://doi.org/10.18637/jss.v028.i08

Irvine, D. R. F. (2010). Plasticity in the auditory pathway. In A. R. Palmer & A. Rees (Eds.), *The Oxford Handbook of Auditory Science: The Auditory Brain* (p. 0). Oxford University Press. https://doi.org/10.1093/oxfordhb/9780199233281.013.0016

Ito, H., & Schuman, E. (2008). Frequency-dependent signal transmission and modulation by neuromodulators. *Frontiers in Neuroscience*, *2*. https://www.frontiersin.org/articles/10.3389/neuro.01.027.2008

Ji, W., Gao, E., & Suga, N. (2001). Effects of Acetylcholine and Atropine on Plasticity of Central Auditory Neurons Caused by Conditioning in Bats. *Journal of Neurophysiology*, *86*(1), 211–225. https://doi.org/10.1152/jn.2001.86.1.211

Ji, W., & Suga, N. (2003). Development of reorganization of the auditory cortex caused by fear conditioning: Effect of atropine. *Journal of Neurophysiology*, *90*(3), 1904–1909. https://doi.org/10.1152/jn.00363.2003

Ji, W., & Suga, N. (2009). Tone-Specific and Nonspecific Plasticity of Inferior Colliculus Elicited by Pseudo-Conditioning: Role of Acetylcholine and Auditory and

Somatosensory Cortices. *Journal of Neurophysiology*, *102*(2), 941–952. https://doi.org/10.1152/jn.00222.2009

Ji, W., Suga, N., & Gao, E. (2005). Effects of Agonists and Antagonists of NMDA and ACh Receptors on Plasticity of Bat Auditory System Elicited by Fear Conditioning. *Journal of Neurophysiology*, *94*(2), 1199–1211. https://doi.org/10.1152/jn.00112.2005

Jones, B. E. (1991). Paradoxical sleep and its chemical/structural substrates in the brain. *Neuroscience*, *40*(3), 637–656. https://doi.org/10.1016/0306-4522(91)90002-6

Jones, E. G. (1975). Some aspects of the organization of the thalamic reticular complex. *The Journal of Comparative Neurology*, *162*(3), 285–308. https://doi.org/10.1002/cne.901620302

Jones, E. G., & Rockel, A. J. (1971). The synaptic organization in the medial geniculate body of afferent fibres ascending from the inferior colliculus. *Zeitschrift Fur Zellforschung Und Mikroskopische Anatomie (Vienna, Austria: 1948)*, *113*(1), 44–66. https://doi.org/10.1007/BF00331201

Joo, K. M., Chung, Y. H., Kim, M. K., Nam, R. H., Lee, B. L., Lee, K. H., & Cha, C. I. (2004). Distribution of vasoactive intestinal peptide and pituitary adenylate cyclase-activating polypeptide receptors (VPAC1, VPAC2, and PAC1 receptor) in the rat brain. *Journal of Comparative Neurology*, *476*(4), 388–413. https://doi.org/10.1002/cne.20231

Kawai, H., Lazar, R., & Metherate, R. (2007). Nicotinic control of axon excitability regulates thalamocortical transmission. *Nature Neuroscience*, *10*(9), 1168–1175. https://doi.org/10.1038/nn1956

Kim, J. j., Gross, J., Potashner, S. j., & Morest, D. k. (2004). Fine structure of long-term changes in the cochlear nucleus after acoustic overstimulation: Chronic degeneration and new

growth of synaptic endings. *Journal of Neuroscience Research*, *77*(6), 817–828. https://doi.org/10.1002/jnr.20212

Knott, V. J., Bolton, K., Heenan, A., Shah, D., Fisher, D. J., & Villeneuve, C. (2009). Effects of acute nicotine on event-related potential and performance indices of auditory distraction in nonsmokers. *Nicotine & Tobacco Research*, *11*(5), 519–530. https://doi.org/10.1093/ntr/ntp044

Knott, V., Shah, D., Millar, A., McIntosh, J., Fisher, D., Blais, C., & Ilivitsky, V. (2012). Nicotine, Auditory Sensory Memory, and sustained Attention in a Human Ketamine Model of Schizophrenia: Moderating Influence of a Hallucinatory Trait. *Frontiers in Pharmacology*, *3*, 172. https://doi.org/10.3389/fphar.2012.00172

Kohlmeier, K. A., & Reiner, P. B. (1999). Vasoactive Intestinal Polypeptide Excites Medial Pontine Reticular Formation Neurons in the Brainstem Rapid Eye Movement Sleep-Induction Zone. *The Journal of Neuroscience*, *19*(10), 4073–4081. https://doi.org/10.1523/JNEUROSCI.19-10-04073.1999

Kozak, R., Bowman, E. M., Latimer, M. P., Rostron, C. L., & Winn, P. (2005). Excitotoxic lesions of the pedunculopontine tegmental nucleus in rats impair performance on a test of sustained attention. *Experimental Brain Research*, *162*(2), 257–264. https://doi.org/10.1007/s00221-004-2143-3

Kreeger, L. J., Connelly, C. J., Mehta, P., Zemelman, B. V., & Golding, N. L. (2021). Excitatory cholecystokinin neurons of the midbrain integrate diverse temporal responses and drive auditory thalamic subdomains. *Proceedings of the National Academy of Sciences of the United States of America*, *118*(10). https://doi.org/10.1073/pnas.2007724118

Kudo, M., & Niimi, K. (1978). Ascending projections of the inferior colliculus onto the medial geniculate body in the cat studied by anterograde and retrograde tracing techniques. *Brain Research*, *155*(1), 113–117. https://doi.org/10.1016/0006-8993(78)90310-4

Kuznetsova, A., Brockhoff, P. B., & Christensen, R. H. B. (2017). lmerTest Package: Tests in Linear Mixed Effects Models. *Journal of Statistical Software*, *82*(1), 1–26. https://doi.org/10.18637/jss.v082.i13

Kwapiszewski, J. T., Rivera-Perez, L. M., & Roberts, M. T. (2023). Cholinergic Boutons are Distributed Along the Dendrites and Somata of VIP Neurons in the Inferior Colliculus. *Journal of the Association for Research in Otolaryngology: JARO*, *24*(2), 181–196. https://doi.org/10.1007/s10162-022-00885-9

Lam, K. S. (1991). Vasoactive intestinal peptide in the hypothalamus and pituitary. *Neuroendocrinology*, *53 Suppl 1*, 45–51. https://doi.org/10.1159/000125795

Lamotte d'Incamps, B., & Ascher, P. (2008). Four Excitatory Postsynaptic Ionotropic Receptors Coactivated at the Motoneuron–Renshaw Cell Synapse. *The Journal of Neuroscience*, *28*(52), 14121–14131. https://doi.org/10.1523/JNEUROSCI.3311-08.2008

Lamotte d'Incamps, B., Zorbaz, T., Dingova, D., Krejci, E., & Ascher, P. (2018). Stoichiometry of the Heteromeric Nicotinic Receptors of the Renshaw Cell. *The Journal of Neuroscience*, *38*(21), 4943–4956. https://doi.org/10.1523/JNEUROSCI.0070-18.2018

Lee, S.-H., & Cox, C. L. (2003). Vasoactive Intestinal Peptide Selectively Depolarizes Thalamic Relay Neurons and Attenuates Intrathalamic Rhythmic Activity. *Journal of Neurophysiology*, *90*(2), 1224–1234. https://doi.org/10.1152/jn.00280.2003

Lin, F. R., Yaffe, K., Xia, J., Xue, Q.-L., Harris, T. B., Purchase-Helzner, E., Satterfield, S., Ayonayon, H. N., Ferrucci, L., Simonsick, E. M., & Health ABC Study Group. (2013).

Hearing loss and cognitive decline in older adults. *JAMA Internal Medicine*, *173*(4), 293–299. https://doi.org/10.1001/jamainternmed.2013.1868

Madisen, L., Zwingman, T. A., Sunkin, S. M., Oh, S. W., Zariwala, H. A., Gu, H., Ng, L. L., Palmiter, R. D., Hawrylycz, M. J., Jones, A. R., Lein, E. S., & Zeng, H. (2010). A robust and high-throughput Cre reporting and characterization system for the whole mouse brain. *Nature Neuroscience*, *13*(1), 133–140. https://doi.org/10.1038/nn.2467

Malmierca, M. S., Blackstad, T. W., Osen, K. K., Karagülle, T., & Molowny, R. L. (1993). The central nucleus of the inferior colliculus in rat: A Golgi and computer reconstruction study of neuronal and laminar structure. *Journal of Comparative Neurology*, *333*(1), 1–27. https://doi.org/10.1002/cne.903330102

Marks, M. J., Whiteaker, P., & Collins, A. C. (2006). Deletion of the α7, β2, or β4 Nicotinic Receptor Subunit Genes Identifies Highly Expressed Subtypes with Relatively Low Affinity for [3H]Epibatidine. *Molecular Pharmacology*, *70*(3), 947–959. https://doi.org/10.1124/mol.106.025338

Marks, M. J., Whiteaker, P., Grady, S. R., Picciotto, M. R., McIntosh, J. M., & Collins, A. C. (2002). Characterization of [125I]epibatidine binding and nicotinic agonist-mediated 86Rb+ efflux in interpeduncular nucleus and inferior colliculus of β2 null mutant mice. *Journal of Neurochemistry*, *81*(5), 1102–1115. https://doi.org/10.1046/j.1471-4159.2002.00910.x

McKay, B. E., Placzek, A. N., & Dani, J. A. (2007). Regulation of Synaptic Transmission and Plasticity by Neuronal Nicotinic Acetylcholine Receptors. *Biochemical Pharmacology*, *74*(8), 1120–1133. https://doi.org/10.1016/j.bcp.2007.07.001

Mellott, J. G., Foster, N. L., Ohl, A. P., & Schofield, B. R. (2014). Excitatory and inhibitory projections in parallel pathways from the inferior colliculus to the auditory thalamus. *Frontiers in Neuroanatomy*, *8*, 124. https://doi.org/10.3389/fnana.2014.00124

Metherate, R., & Cruikshank, S. J. (1999). Thalamocortical inputs trigger a propagating envelope of gamma-band activity in auditory cortex in vitro. *Experimental Brain Research*, *126*(2), 160–174. https://doi.org/10.1007/s002210050726

Mike, A., Castro, N. G., & Albuquerque, E. X. (2000). Choline and acetylcholine have similar kinetic properties of activation and desensitization on the α7 nicotinic receptors in rat hippocampal neurons. *Brain Research*, *882*(1), 155–168. https://doi.org/10.1016/S0006-8993(00)02863-8

Millar, N. S., & Gotti, C. (2009). Diversity of vertebrate nicotinic acetylcholine receptors. *Neuropharmacology*, *56*(1), 237–246. https://doi.org/10.1016/j.neuropharm.2008.07.041

Montero, V. M. (1983). Ultrastructural identification of axon terminals from the thalamic reticular nucleus in the medial geniculate body in the rat: An EM autoradiographic study. *Experimental Brain Research*, *51*(3), 338–342. https://doi.org/10.1007/BF00237870

Moore, D. R., & Kowalchuk, N. E. (1988). Auditory brainstem of the ferret: Effects of unilateral cochlear lesions on cochlear nucleus volume and projections to the inferior colliculus. *Journal of Comparative Neurology*, *272*(4), 503–515. https://doi.org/10.1002/cne.902720405

Morley, B. J., & Happe, H. K. (2000). Cholinergic receptors: Dual roles in transduction and plasticity. *Hearing Research*, *147*(1), 104–112. https://doi.org/10.1016/S0378-5955(00)00124-6

Mossop, J. E., Wilson, M. J., Caspary, D. M., & Moore, D. R. (2000). Down-regulation of inhibition following unilateral deafening. *Hearing Research*, *147*(1), 183–187. https://doi.org/10.1016/S0378-5955(00)00054-X

Motts, S. D., & Schofield, B. R. (2009). Sources of cholinergic input to the inferior colliculus. *Neuroscience*, *160*(1), 103–114. https://doi.org/10.1016/j.neuroscience.2009.02.036

Murphy, P. C., Grieve, K. L., & Sillito, A. M. (1993). Effects of vasoactive intestinal polypeptide on the response properties of cells in area 17 of the cat visual cortex. *Journal of Neurophysiology*, *69*(5), 1465–1474. https://doi.org/10.1152/jn.1993.69.5.1465

Noftz, W. A., Beebe, N. L., Mellott, J. G., & Schofield, B. R. (2020). Cholinergic Projections From the Pedunculopontine Tegmental Nucleus Contact Excitatory and Inhibitory Neurons in the Inferior Colliculus. *Frontiers in Neural Circuits*, *14*. https://doi.org/10.3389/fncir.2020.00043

Oliver, D. L., & Morest, D. K. (1984). The central nucleus of the inferior colliculus in the cat. *Journal of Comparative Neurology*, *222*(2), 237–264. https://doi.org/10.1002/cne.902220207

Papke, R. L., Dwoskin, L. P., Crooks, P. A., Zheng, G., Zhang, Z., McIntosh, J. M., & Stokes, C. (2008). Extending the analysis of nicotinic receptor antagonists with the study of alpha6 nicotinic receptor subunit chimeras. *Neuropharmacology*, *54*(8), 1189–1200. https://doi.org/10.1016/j.neuropharm.2008.03.010

Papke, R. L., Meyer, E., Nutter, T., & Uteshev, V. V. (2000). A7 Receptor-selective agonists and modes of α7 receptor activation. *European Journal of Pharmacology*, *393*(1), 179–195. https://doi.org/10.1016/S0014-2999(00)00009-1

Papke, R. L., Sanberg, P. R., & Shytle, R. D. (2001). Analysis of Mecamylamine Stereoisomers on Human Nicotinic Receptor Subtypes. *Journal of Pharmacology and Experimental Therapeutics*, *297*(2), 646–656.

Papke, R. L., Wecker, L., & Stitzel, J. A. (2010). Activation and Inhibition of Mouse Muscle and Neuronal Nicotinic Acetylcholine Receptors Expressed in Xenopus Oocytes. *The Journal of Pharmacology and Experimental Therapeutics*, *333*(2), 501–518. https://doi.org/10.1124/jpet.109.164566

Peruzzi, D., Bartlett, E., Smith, P. H., & Oliver, D. L. (1997). A Monosynaptic GABAergic Input from the Inferior Colliculus to the Medial Geniculate Body in Rat. *The Journal of Neuroscience*, *17*(10), 3766–3777. https://doi.org/10.1523/JNEUROSCI.17-10-03766.1997

Pham, C. Q., Kapolowicz, M. R., Metherate, R., & Zeng, F.-G. (2020). Nicotine enhances auditory processing in healthy and normal-hearing young adult nonsmokers. *Psychopharmacology*, *237*(3), 833–840. https://doi.org/10.1007/s00213-019-05421-x

Popper, A. N., & Fay, R. R. (Eds.). (1992). *The Mammalian Auditory Pathway: Neurophysiology* (Vol. 2). Springer. https://doi.org/10.1007/978-1-4612-2838-7

Prysor-Jones, R. A., & Jenkins, J. S. (1988). Vasoactive intestinal peptide and anterior pituitary function. *Clinical Endocrinology*, *29*(6), 677–688. https://doi.org/10.1111/j.1365-2265.1988.tb03716.x

Pugh, P. C., Jayakar, S. S., & Margiotta, J. F. (2010). PACAP/PAC1R signaling modulates acetylcholine release at neuronal nicotinic synapses. *Molecular and Cellular Neurosciences*, *43*(2), 244. https://doi.org/10.1016/j.mcn.2009.11.007

Rank, M. M., Murray, K. C., Stephens, M. J., D'Amico, J., Gorassini, M. A., & Bennett, D. J. (2011). Adrenergic Receptors Modulate Motoneuron Excitability, Sensory Synaptic Transmission and Muscle Spasms After Chronic Spinal Cord Injury. *Journal of Neurophysiology*, *105*(1), 410–422. https://doi.org/10.1152/jn.00775.2010

Rees, C. L., Moradi, K., & Ascoli, G. A. (2017). Weighing the Evidence in Peters' Rule: Does Neuronal Morphology Predict Connectivity? *Trends in Neurosciences*, *40*(2), 63–71. https://doi.org/10.1016/j.tins.2016.11.007

Reese, N. B., Garcia-Rill, E., & Skinner, R. D. (1995a). Auditory input to the pedunculopontine nucleus: I. Evoked potentials. *Brain Research Bulletin*, *37*(3), 257–264. https://doi.org/10.1016/0361-9230(95)00002-V

Reese, N. B., Garcia-Rill, E., & Skinner, R. D. (1995b). Auditory input to the pedunculopontine nucleus: II. Unit responses. *Brain Research Bulletin*, *37*(3), 265–273. https://doi.org/10.1016/0361-9230(95)00001-U

Regehr, W. G., Carey, M. R., & Best, A. R. (2009). Activity-Dependent Regulation of Synapses by Retrograde Messengers. *Neuron*, *63*(2), 154–170. https://doi.org/10.1016/j.neuron.2009.06.021

Rice, M. E., & Cragg, S. J. (2004). Nicotine amplifies reward-related dopamine signals in striatum. *Nature Neuroscience*, *7*(6), 583–584. https://doi.org/10.1038/nn1244

Robertson, D., & Irvine, D. R. F. (1989). Plasticity of frequency organization in auditory cortex of guinea pigs with partial unilateral deafness. *Journal of Comparative Neurology*, *282*(3), 456–471. https://doi.org/10.1002/cne.902820311

Rosen, S., Susswein, A., Cropper, E., Weiss, K., & Kupfermann, I. (1989). Selective modulation of spike duration by serotonin and the neuropeptides, FMRFamide, SCPB, buccalin and

myomodulin in different classes of mechanoafferent neurons in the cerebral ganglion of Aplysia. *The Journal of Neuroscience*, *9*(2), 390–402. https://doi.org/10.1523/JNEUROSCI.09-02-00390.1989

Rossi, J., Balthasar, N., Olson, D., Scott, M., Berglund, E., Lee, C. E., Choi, M. J., Lauzon, D., Lowell, B. B., & Elmquist, J. K. (2011). Melanocortin-4-receptors Expressed by Cholinergic Neurons Regulate Energy Balance and Glucose Homeostasis. *Cell Metabolism*, *13*(2), 195–204. https://doi.org/10.1016/j.cmet.2011.01.010

Rouiller, E. M., Colomb, E., Capt, M., & De Ribaupierre, F. (1985). Projections of the reticular complex of the thalamus onto physiologically characterized regions of the medial geniculate body. *Neuroscience Letters*, *53*(2), 227–232. https://doi.org/10.1016/0304-3940(85)90190-9

Rouiller, E. M., & de Ribaupierre, F. (1985). Origin of afferents to physiologically defined regions of the medial geniculate body of the cat: Ventral and dorsal divisions. *Hearing Research*, *19*(2), 97–114. https://doi.org/10.1016/0378-5955(85)90114-5

Sakai, K. (2012). Discharge properties of presumed cholinergic and noncholinergic laterodorsal tegmental neurons related to cortical activation in non-anesthetized mice. *Neuroscience*, *224*, 172–190. https://doi.org/10.1016/j.neuroscience.2012.08.032

Sakurai, A., Darghouth, N. R., Butera, R. J., & Katz, P. S. (2006). Serotonergic Enhancement of a 4-AP-Sensitive Current Mediates the Synaptic Depression Phase of Spike Timing-Dependent Neuromodulation. *The Journal of Neuroscience*, *26*(7), 2010–2021. https://doi.org/10.1523/JNEUROSCI.2599-05.2006

Salas, R., Cook, K. D., Bassetto, L., & De Biasi, M. (2004). The α3 and β4 nicotinic acetylcholine receptor subunits are necessary for nicotine-induced seizures and

hypolocomotion in mice. *Neuropharmacology*, *47*(3), 401–407. https://doi.org/10.1016/j.neuropharm.2004.05.002

Salas, R., Pieri, F., Fung, B., Dani, J. A., & De Biasi, M. (2003). Altered Anxiety-Related Responses in Mutant Mice Lacking the β4 Subunit of the Nicotinic Receptor. *The Journal of Neuroscience*, *23*(15), 6255–6263. https://doi.org/10.1523/JNEUROSCI.23-15-06255.2003

Saldaña, E., Feliciano, M., & Mugnaini, E. (1996). Distribution of descending projections from primary auditory neocortex to inferior colliculus mimics the topography of intracollicular projections. *Journal of Comparative Neurology*, *371*(1), 15–40. https://doi.org/10.1002/(SICI)1096-9861(19960715)371:1<15::AID-CNE2>3.0.CO;2-O

Schofield, B. R. (2010). Projections from auditory cortex to midbrain cholinergic neurons that project to the inferior colliculus. *Neuroscience*, *166*(1), 231. https://doi.org/10.1016/j.neuroscience.2009.12.008

Schofield, B. R., & Motts, S. D. (2009). Projections from auditory cortex to cholinergic cells in the midbrain tegmentum of guinea pigs. *Brain Research Bulletin*, *80*(3), 163–170. https://doi.org/10.1016/j.brainresbull.2009.06.015

Schofield, B. R., Motts, S. D., & Mellott, J. G. (2011). Cholinergic Cells of the Pontomesencephalic Tegmentum: Connections with Auditory Structures from Cochlear Nucleus to Cortex. *Hearing Research*, *279*(1–2), 85–95. https://doi.org/10.1016/j.heares.2010.12.019

Scholze, P., & Huck, S. (2020). The α5 Nicotinic Acetylcholine Receptor Subunit Differentially Modulates α4β2* and α3β4* Receptors. *Frontiers in Synaptic Neuroscience*, *12*. https://doi.org/10.3389/fnsyn.2020.607959

Scholze, P., Koth, G., Orr-Urtreger, A., & Huck, S. (2012). Subunit composition of α5-containing nicotinic receptors in the rodent habenula. *Journal of Neurochemistry*, *121*(4), 551–560. https://doi.org/10.1111/j.1471-4159.2012.07714.x

Schwartz, R. D. (1986). Autoradiographic distribution of high affinity muscarinic and nicotinic cholinergic receptors labeled with [3H]acetylcholine in rat brain. *Life Sciences*, *38*(23), 2111–2119. https://doi.org/10.1016/0024-3205(86)90210-9

Sheffield, E. B., Quick, M. W., & Lester, R. A. J. (2000). Nicotinic acetylcholine receptor subunit mRNA expression and channel function in medial habenula neurons. *Neuropharmacology*, *39*(13), 2591–2603. https://doi.org/10.1016/S0028-3908(00)00138-6

Sheward, W. J., Lutz, E. M., & Harmar, A. J. (1995). The distribution of vasoactive intestinal peptide2 receptor messenger RNA in the rat brain and pituitary gland as assessed by in situ hybridization. *Neuroscience*, *67*(2), 409–418. https://doi.org/10.1016/0306-4522(95)00048-N

Silveira, M. A., Anair, J. D., Beebe, N. L., Mirjalili, P., Schofield, B. R., & Roberts, M. T. (2020). Neuropeptide Y Expression Defines a Novel Class of GABAergic Projection Neuron in the Inferior Colliculus. *The Journal of Neuroscience*, *40*(24), 4685–4699. https://doi.org/10.1523/JNEUROSCI.0420-20.2020

Smucny, J., Olincy, A., Rojas, D. C., & Tregellas, J. R. (2016). Neuronal effects of nicotine during auditory selective attention in schizophrenia. *Human Brain Mapping*, *37*(1), 410–421. https://doi.org/10.1002/hbm.23040

Sottile, S. Y., Hackett, T. A., Cai, R., Ling, L., Llano, D. A., & Caspary, D. M. (2017). Presynaptic Neuronal Nicotinic Receptors Differentially Shape Select Inputs to Auditory

Thalamus and Are Negatively Impacted by Aging. *The Journal of Neuroscience: The Official Journal of the Society for Neuroscience*, *37*(47), 11377–11389. https://doi.org/10.1523/JNEUROSCI.1795-17.2017

Stokes, C., & Papke, R. L. (2012). Use of an α3-β4 nicotinic acetylcholine receptor subunit concatamer to characterize ganglionic receptor subtypes with specific subunit composition reveals species-specific pharmacologic properties. *Neuropharmacology*, *63*(4), 538–546. https://doi.org/10.1016/j.neuropharm.2012.04.035

Strasser, H., & Weber, C. (1999). *On the Asymptotic Theory of Permutation Statistics* (Paper No. 27). SFB Adaptive Information Systems and Modelling in Economics and Management Science, WU Vienna University of Economics and Business. https://epub.wu.ac.at/102/

Sun, Q.-Q., Prince, D. A., & Huguenard, J. R. (2003). Vasoactive intestinal polypeptide and pituitary adenylate cyclase-activating polypeptide activate hyperpolarization-activated cationic current and depolarize thalamocortical neurons in vitro. *The Journal of Neuroscience: The Official Journal of the Society for Neuroscience*, *23*(7), 2751–2758.

Sun, R., Zhang, W., Bo, J., Zhang, Z., Lei, Y., Huo, W., Liu, Y., Ma, Z., & Gu, X. (2017). Spinal activation of alpha7-nicotinic acetylcholine receptor attenuates posttraumatic stress disorder-related chronic pain via suppression of glial activation. *Neuroscience*, *344*, 243–254. https://doi.org/10.1016/j.neuroscience.2016.12.029

Syka, J., Popelár, J., Kvasnák, E., & Astl, J. (2000). Response properties of neurons in the central nucleus and external and dorsal cortices of the inferior colliculus in guinea pig. *Experimental Brain Research*, *133*(2), 254–266. https://doi.org/10.1007/s002210000426

Takahashi, T., Yoshida, T., Harada, K., Miyagi, T., Hashimoto, K., Hide, I., Tanaka, S., Irifune, M., & Sakai, N. (2020). Component of nicotine-induced intracellular calcium elevation

mediated through α3- and α5-containing nicotinic acetylcholine receptors are regulated by cyclic AMP in SH-SY 5Y cells. *PLoS ONE*, *15*(11), e0242349. https://doi.org/10.1371/journal.pone.0242349

Takeuchi, S., Kawanai, T., Yamauchi, R., Chen, L., Miyaoka, T., Yamada, M., Asano, S., Hayata-Takano, A., Nakazawa, T., Yano, K., Horiguchi, N., Nakagawa, S., Takuma, K., Waschek, J. A., Hashimoto, H., & Ago, Y. (2020). Activation of the VPAC2 Receptor Impairs Axon Outgrowth and Decreases Dendritic Arborization in Mouse Cortical Neurons by a PKA-Dependent Mechanism. *Frontiers in Neuroscience*, *14*. https://www.frontiersin.org/articles/10.3389/fnins.2020.00521

Taniguchi, H., He, M., Wu, P., Kim, S., Paik, R., Sugino, K., Kvitsiani, D., Kvitsani, D., Fu, Y., Lu, J., Lin, Y., Miyoshi, G., Shima, Y., Fishell, G., Nelson, S. B., & Huang, Z. J. (2011). A resource of Cre driver lines for genetic targeting of GABAergic neurons in cerebral cortex. *Neuron*, *71*(6), 995–1013. https://doi.org/10.1016/j.neuron.2011.07.026

Usdin, T. B., Bonner, T. I., & Mezey, E. (1994). Two receptors for vasoactive intestinal polypeptide with similar specificity and complementary distributions. *Endocrinology*, *135*(6), 2662–2680. https://doi.org/10.1210/endo.135.6.7988457

Vertongen, P., Schiffmann, S. N., Gourlet, P., & Robberecht, P. (1997). Autoradiographic Visualization of the Receptor Subclasses for Vasoactive Intestinal Polypeptide (VIP) in Rat Brain. *Peptides*, *18*(10), 1547–1554. https://doi.org/10.1016/S0196-9781(97)00229-5

Wada, E., Wada, K., Boulter, J., Deneris, E., Heinemann, S., Patrick, J., & Swanson, L. W. (1989). Distribution of alpha 2, alpha 3, alpha 4, and beta 2 neuronal nicotinic receptor subunit mRNAs in the central nervous system: A hybridization histochemical study in the

rat. *The Journal of Comparative Neurology*, *284*(2), 314–335. https://doi.org/10.1002/cne.902840212

Wang, F., Gerzanich, V., Wells, G. B., Anand, R., Peng, X., Keyser, K., & Lindstrom, J. (1996). Assembly of Human Neuronal Nicotinic Receptor α5 Subunits with α3, β2, and β4 Subunits *. *Journal of Biological Chemistry*, *271*(30), 17656–17665. https://doi.org/10.1074/jbc.271.30.17656

Wang, H.-L., Li, A., & Wu, T. (1997). Vasoactive intestinal polypeptide enhances the GABAergic synaptic transmission in cultured hippocampal neurons. *Brain Research*, *746*(1), 294–300. https://doi.org/10.1016/S0006-8993(96)00772-X

Watanabe, T., & Simada, Z. (1973). Pharmacological properties of cat's collicular auditory neurons. *The Japanese Journal of Physiology*, *23*(3), 291–308. https://doi.org/10.2170/jjphysiol.23.291

Whiteaker, P., Peterson, C. G., Xu, W., McIntosh, J. M., Paylor, R., Beaudet, A. L., Collins, A. C., & Marks, M. J. (2002). Involvement of the α3 Subunit in Central Nicotinic Binding Populations. *The Journal of Neuroscience*, *22*(7), 2522–2529. https://doi.org/10.1523/JNEUROSCI.22-07-02522.2002

Winer, J. A., Larue, D. T., Diehl, J. J., & Hefti, B. J. (1998). Auditory cortical projections to the cat inferior colliculus. *Journal of Comparative Neurology*, *400*(2), 147–174. https://doi.org/10.1002/(SICI)1096-9861(19981019)400:2<147::AID-CNE1>3.0.CO;2-9

Winer, J. A., & Schreiner, C. E. (Eds.). (2005). *The Inferior Colliculus*. Springer. https://doi.org/10.1007/b138578

Wonnacott, S. (1997). Presynaptic nicotinic ACh receptors. *Trends in Neurosciences*, *20*(2), 92–98. https://doi.org/10.1016/s0166-2236(96)10073-4

Zaveri, N., Jiang, F., Olsen, C., Polgar, W., & Toll, L. (2010). Novel alpha3beta4 nicotinic acetylcholine receptor-selective ligands. Discovery, structure-activity studies and pharmacological evaluation. *Journal of Medicinal Chemistry*, *53*(22), 8187–8191. https://doi.org/10.1021/jm1006148

Zhang, C., Beebe, N. L., Schofield, B. R., Pecka, M., & Burger, R. M. (2021). Endogenous Cholinergic Signaling Modulates Sound-Evoked Responses of the Medial Nucleus of the Trapezoid Body. *The Journal of Neuroscience: The Official Journal of the Society for Neuroscience*, *41*(4), 674–688. https://doi.org/10.1523/JNEUROSCI.1633-20.2020

Zhang, H., & Sulzer, D. (2004). Frequency-dependent modulation of dopamine release by nicotine. *Nature Neuroscience*, *7*(6), 581–582. https://doi.org/10.1038/nn1243

Zhang, L., Wu, C., Martel, D. T., West, M., Sutton, M. A., & Shore, S. E. (2019). Remodeling of cholinergic input to the hippocampus after noise exposure and tinnitus induction in guinea pigs. *Hippocampus*, *29*(8), 669–682. https://doi.org/10.1002/hipo.23058

Zheng, Q. Y., Johnson, K. R., & Erway, L. C. (1999). Assessment of hearing in 80 inbred strains of mice by ABR threshold analyses. *Hearing Research*, *130*(1–2), 94–107. https://doi.org/10.1016/s0378-5955(99)00003-9